



OPEN ACCESS

EDITED BY

Hu Wang,
Southwest Jiaotong University, China

REVIEWED BY

Jianzhang Pang,
Institute of Geology, China Earthquake
Administration, China
Xibin Tan,
Institute of Geology, China Earthquake
Administration, China
Xi Chen,
China University of Geosciences, China

*CORRESPONDENCE

Zhiwu Li,
✉ lizhiwu06@mail.cdut.edu.cn

SPECIALTY SECTION

This article was submitted to Structural
Geology and Tectonics,
a section of the journal
Frontiers in Earth Science

RECEIVED 01 December 2022

ACCEPTED 03 January 2023

PUBLISHED 06 February 2023

CITATION

Wang Z, Li Z, Ran B, Liu S, Wu W, Ye Y,
Tong K, Hua T and Li J (2023), Mid-
cretaceous rapid denudation of Eastern
Tibetan plateau: Insights from detrital
records at the Southwestern corner of
Sichuan basin.
Front. Earth Sci. 11:1113377.
doi: 10.3389/feart.2023.1113377

COPYRIGHT

© 2023 Wang, Li, Ran, Liu, Wu, Ye, Tong,
Hua and Li. This is an open-access article
distributed under the terms of the [Creative
Commons Attribution License \(CC BY\)](https://creativecommons.org/licenses/by/4.0/).
The use, distribution or reproduction in
other forums is permitted, provided the
original author(s) and the copyright
owner(s) are credited and that the original
publication in this journal is cited, in
accordance with accepted academic
practice. No use, distribution or
reproduction is permitted which does not
comply with these terms.

Mid-cretaceous rapid denudation of Eastern Tibetan plateau: Insights from detrital records at the Southwestern corner of Sichuan basin

Zijian Wang¹, Zhiwu Li^{1*}, Bo Ran¹, Shugen Liu^{1,2}, Wenhui Wu¹, Yuehao Ye¹, Kui Tong¹, Tian Hua¹ and Jinxi Li¹

¹State Key Laboratory of Oil and Gas Reservoir Geology and Exploitation, Chengdu University of Technology, Chengdu, China, ²Xihua University, Chengdu, Sichuan, China

Reconstruction of the Cretaceous tectonic evolution of the eastern margin of the Tibetan Plateau is of great significance to understanding the formation and early evolution of the Tibetan Plateau. The thick late Mesozoic sedimentary sequence in the Western Sichuan Basin may record the evolution of the basin itself and the tectonic uplift history of the eastern margin of the Tibetan Plateau during the Cretaceous period. Here we provide new multi-proxy provenance data from conglomerate clast populations, sandstone petrography, heavy mineral assemblages, U-Pb dating of detrital zircon, paleocurrent data, and detrital garnet geochemistry from the Cretaceous clastic units in the southwest corner of Sichuan Basin. Our analysis reveals two distinct changes in sediment provenance recorded in the Cretaceous strata at the southwest corner of the Sichuan Basin. The first significant change of detrital provenance was identified in the mid-Cretaceous Jiaguan Formation. Metamorphic rocks and volcanic rocks clast, as well as feldspar and mica, increased significantly, a heavy mineral assemblage dominated by hematite–limonite and ilmenite with high ATi and RuZi and low ZTR values, predominantly type Bi garnet and mostly 164 Ma, 207 Ma, 440 Ma, 780 Ma–824 Ma, and 1840 Ma detrital zircon ages, interpreted to be sourced from the Songpan-Ganzi fold belt and Longmenshan orogenic belt. The second shift, in the Guankou Formation, is marked by a low compositional maturity, a distinct increase in fossiliferous carbonate clasts and high GZi index with type Bii garnet, and Triassic zircon ages, indicating the exhumation of Longmenshan orogenic belt during the late Cretaceous. These data collectively indicate that the significant surface uplift and rapid denudation of the eastern margin of the Tibetan Plateau were probably initiated in the mid-Cretaceous (~120 Ma). In conclusion, a detailed hands-on provenance analysis of the clastic sedimentary sequences in the southwest corner of the Sichuan Basin enabled us to determine catchment areas and shifts hitherto unstudied, thus contributing to the exhumation history of the eastern margin of the Tibetan Plateau.

KEYWORDS

Cretaceous denudation, detrital zircon dating, heavy mineral analysis, detrital garnet geochemistry, eastern Tibetan plateau, Sichuan basin

1 Introduction

The surface uplift and growth mechanism of the Tibetan Plateau is a research hotspot (Fielding, 1996; Chung et al., 1998; Mulch and Chamberlain, 2006; Rowley and Currie, 2006; Wang et al., 2008; Rohrmann et al., 2012; Ding et al., 2017, 2022; Spicer et al., 2021). Due to the special tectonic position and unique geological structure and structural characteristics of the eastern Tibetan Plateau (Figure 1), its tectonic evolution history is of great significance to reveal the early uplift and growth of the plateau and its dynamic mechanism (Lin et al., 1996; Harrowfield and Wilson, 2005; Li et al., 2008; Li et al., 2010b; Liu et al., 2019), and has become an important research field. Numerous studies have been conducted on the tectonic uplift history of the eastern Tibetan Plateau in the past decades. However, most of the previous studies have only been concentrated on tectonic uplift history studies on the early Late Mesozoic (Late Triassic—early Jurassic) and Cenozoic (Wang et al., 2012; Tian et al., 2013, 2014a, Tian et al., 2018; Tan et al., 2017; Shen et al., 2019; Tan et al., 2019; Yang et al., 2019), while the tectonic evolution history of the Late Mesozoic (Middle and Late Jurassic—Cretaceous), especially the Cretaceous period, remains unclear (Xue et al., 2017; Wang et al., 2021), hindering our understanding of the early formation and evolution of the Tibetan Plateau.

In recent years, low-temperature thermochronology studies have shown that the Songpan—Ganzi fold belt experienced regional uplift and denudation in Late Jurassic—Early Cretaceous (Tian et al., 2014b) and rapid uplift in the Middle-Late Cretaceous (Kamp et al., 2013; Liu et al., 2019; Yang et al., 2019). Influenced by the remote effect of the Lhasa—Qiangtang terrane collision, the inherited structures of the Longmenshan orogenic belt were reactivated (Arne et al., 1997; Wallis et al., 2003; Roger et al., 2004, 2010; Airaghi, 2017a; Airaghi et al., 2017b, 2018) and denudated significantly during the Cretaceous (Xu et al., 2007, Xu et al., 2016; Airaghi et al., 2018; Xue et al., 2021). In addition, more and more information indicated that there was a significant erosion event in the eastern margin of the Tibetan Plateau in the Middle Cretaceous (Xu and Kamp, 2000; Reid et al., 2005; Kamp et al., 2013; Tian et al., 2014b; Airaghi, 2017a; Liu-Zeng et al., 2018; Liu et al., 2019; Yang et al., 2019). The accumulated denudation thickness is more than 5,000 m, which should be uplifted in a large area and form obvious high terrain (Liu et al., 2019). Thus, the results of thermochronology indicate that the early plateauing of the eastern Plateau began at least during the Cretaceous period prior to the India-Asia collision and produced a large amount of denudative material (Xu et al., 2016; Liu et al., 2019), but the whereabouts of these detritus is unknown. The tectonic uplift in the eastern margin of the Tibetan Plateau and the coupled subsidence of the adjacent sedimentary basins fundamentally control the evolution of the topography, geomorphology, drainage system, and sourcing-sink system in the eastern Tibetan Plateau. However, there are still many controversies about the sedimentary filling process of the Cretaceous basins on the eastern edge of the Tibetan Plateau, as well as the source-sink system associated with its early uplift denudation.

Precambrian basement complex code: KD, Kangdian; BX, Baoxing; PG, Pengguan; XLB, Xuelongbao; JZD, Jiaoziding; MCS, Micang Shan; HN, Hannan. Suture zone code: SDS, Shangdan; AMS, Anyemaqen; MLS, Mianlve; GLS, Ganzi—Litang; JSJS, Jinshajiang; BNS, Banggong—Nujiang. Fault zone code: NQLF, North Qinling; LPSF, Liupanshan; TBF, Tianshui—Baoji; WQLF, West Qinling;

HMF, Hezuo-Minxian; DZF, Dieshan-Zhouqu; EKLf, East Kunlun; MJF, Minjiang; LRF, Longriba; QCF, Qingchuan; WMF, Wenchuan—Maoxian; YBF, Yingxiu—Beichuan; GAF, Guanxian—Anxian; XSHF, Xianshuihe; ANHF, Anlinghe; DLSF, Daliangshan; ZMHF, Zemuhe; XJF, Xiaojiang. Construction unit Code: LMS, Longmenshan orogenic belt; KQQ, Kunlun—Qilian—Qinling composite orogenic belt; HXSG, Hoh Xil—Songpan—Ganzi terrane; YD, Yidun Terrane; NQT, North Qiangtang terrane; SQT, South Qiangtang terrane; LS, Lhasa terrane; HM, Himalayan terrane.

Sediments deposited in the sedimentary basin provide key information about paleo-tectonic events during orogenic development (Baral et al., 2017). Detailed analysis of these basin sediments allows one to trace them back to their original provenance and reconstruct uplift events (DeCelles and Giles, 1996; Jian et al., 2013) and the contemporaneous orogenic exhumation processes (Pettijohn et al., 1987; Najman and Garzanti, 2000; Weltje and Eynatten, 2004; Panaiotu et al., 2007; Rahl et al., 2018). In the past several decades, U-Pb dating based on detrital zircon (chemically stable and mechanically durable within different depositional environments and weathering conditions) (e.g., Veevers & Saeed, 2013; Gehrels, 2014; Allen, 2017) combined with heavy mineral assemblage analysis and single mineral geochemistry from clastic rocks in the basin (Hartley & Otava, 2001; Linka & Stawikowski, 2013; Morton & Hallsworth, 1994 and references therein; Morton et al., 2016) has become a precise tool for provenance analysis and for paleogeography and paleotectonic reconstruction (Dickinson and Suczek, 1979; Dickinson, 1988; Cawood and Nemchin, 2000; Cawood et al., 2012).

Sichuan Basin is the largest Mesozoic sedimentary basin in the Upper Yangtze plate, adjoining the eastern Tibetan Plateau (Figure 1), which is an ideal place to provide crucial information about the formation and depositional history of the basin itself and the tectonic evolution of the eastern Tibetan Plateau (Guo et al., 1996; Lin et al., 1996; Liu et al., 2003; Li et al., 2016a; Li et al., 2016b). Near the entire NE—SW-trending Longmenshan orogenic belt was deposited over 4 km of Late Triassic to Late Cretaceous foreland basin sedimentary rocks (BGMRSF, 1991; Liu, 2006), which are exposed along the eastern margin of the orogenic belt front. This sequence has been used to study the rate of sedimentation and exhumation history of the source region, climatic changes, and paleogeography, and for provenance analysis (Meng et al., 2005; Li et al., 2018; Zhu et al., 2016). So far, previous provenance analysis of the Western Sichuan basin deposits mainly focused on the Upper Triassic Xujiahe Formation (Deng et al., 2008; Li et al., 2010a; Chen et al., 2011; Luo et al., 2014; Zhang et al., 2015; Shao et al., 2016; Zhu et al., 2017; Yan et al., 2019; Mu et al., 2019; Chen et al., 2020), Lower Jurassic Batiaba Formation (Qian et al., 2015; Shao et al., 2016; Tian, 2018; Lv et al., 2022), Middle-Late Jurassic Shaoximiao Formation, Sunning Formation and Penglaizhen Formation (Li et al., 2010a; Yang et al., 2010; Luo et al., 2014; Qian et al., 2015; Li et al., 2018), Lower Cretaceous Chengqiangyan Group of the northwest basin (Li et al., 2016b; Li et al., 2018), Late Cretaceous Wotoushan to Gaokanba Formation, and Paleogene Liujia Formation in the Yibin-Liujia area of the southwest Sichuan Basin (Deng et al., 2018; Jiang et al., 2019), and few investigations have been conducted on the Cretaceous red beds based on the age of U-Pb in zircons (Li et al., 2018) in the southwestern corner of the Sichuan Basin (SWCSB) where the largest accumulations of foreland basin

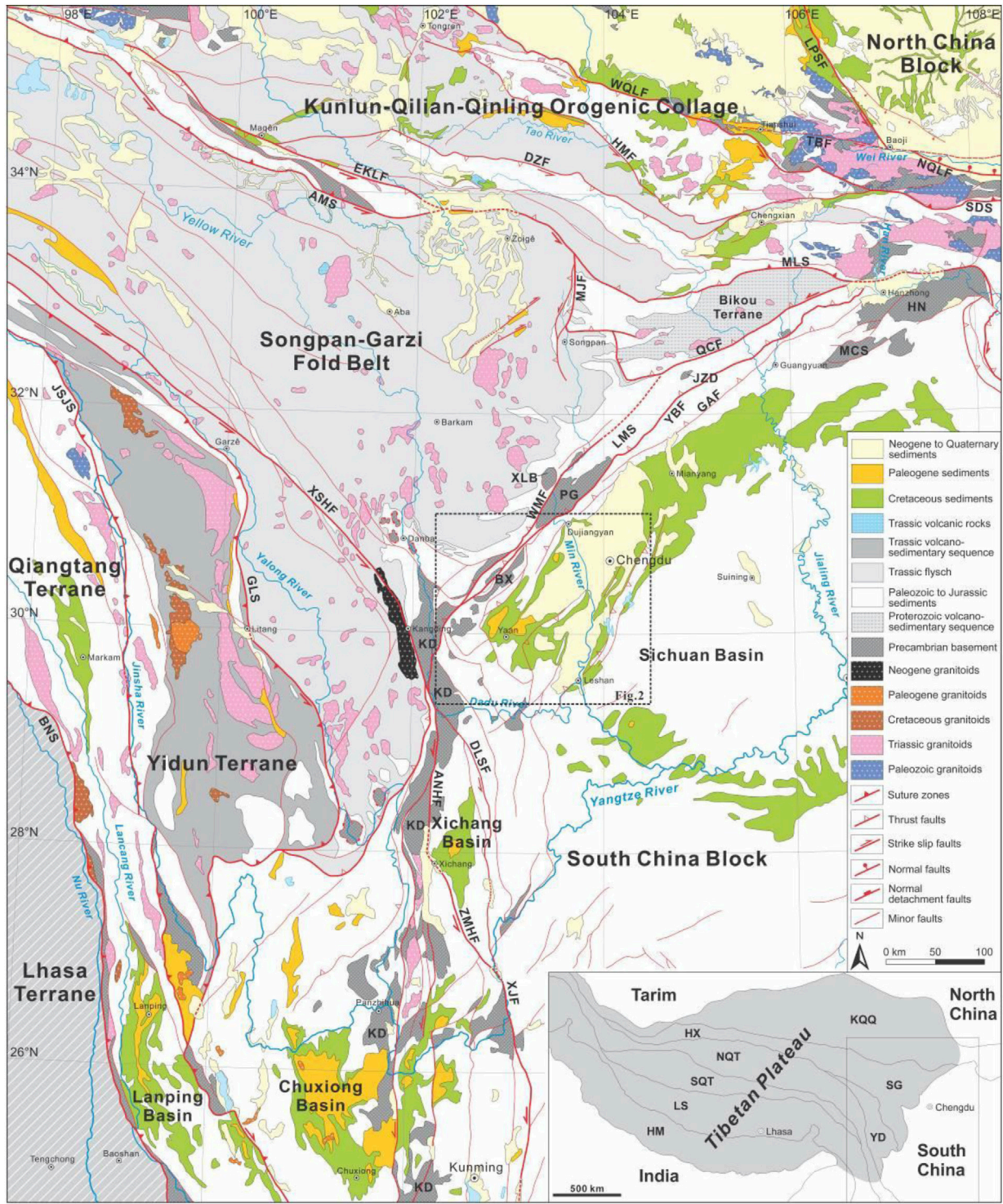


FIGURE 1 Simplified geological and structural map of the eastern Tibetan Plateau (after Liu et al., 2019).

syntectonic deposits are preserved (Figure 2). Meanwhile, it has been suggested that Cretaceous sediments of the southwest Sichuan Basin were supplied by multiple sources systems, and a single U-Pb age component can contribute to multiple potential provenance regions (Li et al., 2018), but the relative contribution of each source region cannot be quantified.

Due to the lack of constraints of other provenance indexes, the precise provenance of these sediments remains unclear, which seriously restricts our understanding of source areas' tectonic events and basin evolution during the Cretaceous. Given that the deposition of the Tianmashan, Jiaguan, and Guankou Formations records key information in the Cretaceous of the Sichuan Basin, it

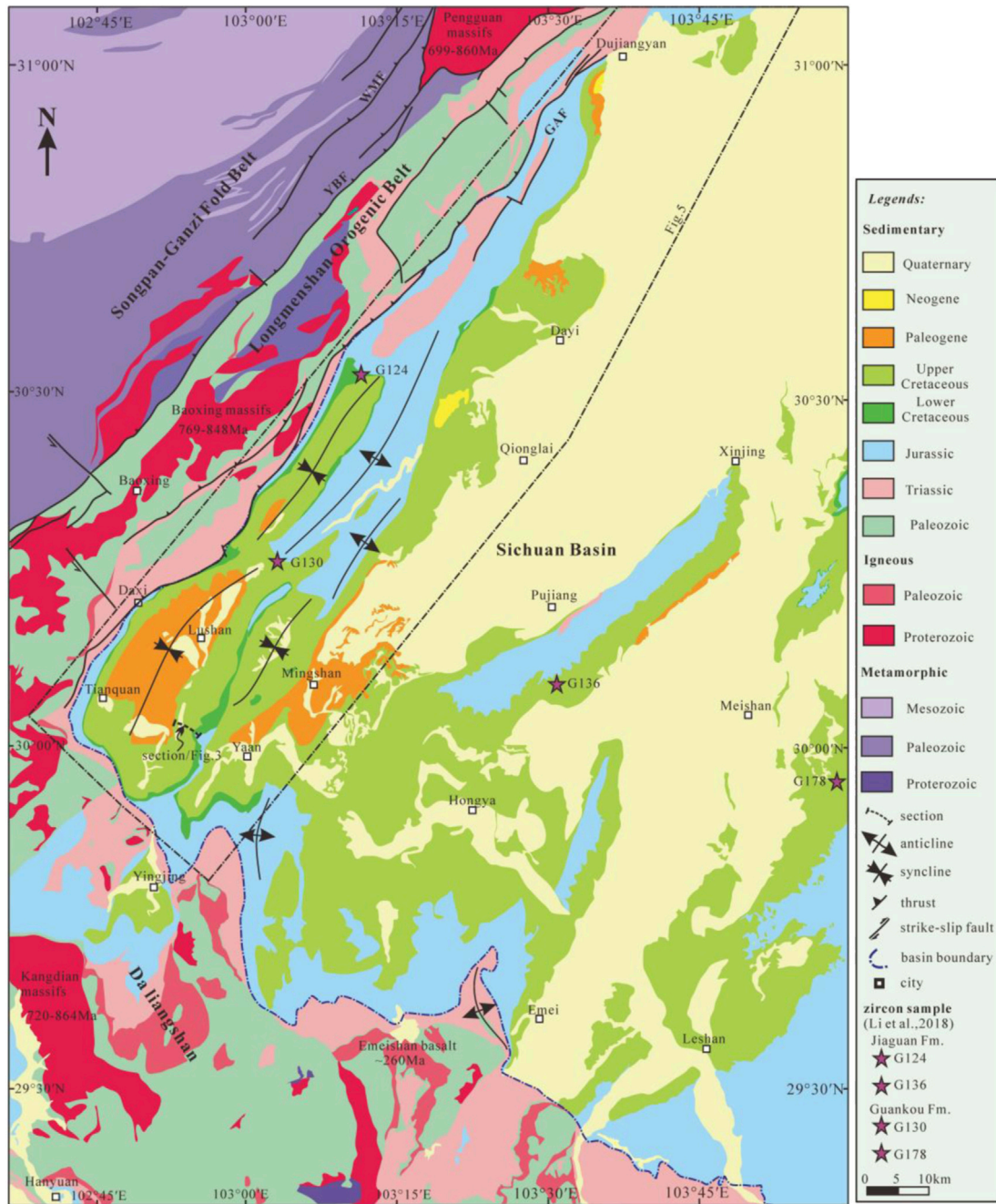


FIGURE 2
 Geological map of the southwestern corner of the Sichuan basin showing the location of measured sections and sampling localities. Geology map modified after Burchfiel et al. (1995), 1:200,000 geologic maps (Ministry of Geology and Mineral Resources, 1991), and our own observations. WMF- Wenchuan-maoxian fault; YBF- Yinxiu-Beichuan fault; GAF- Guanxian-Anxian fault.

requires further research. This comprehensive analysis of multi-proxy provenance will help to overcome the multiple solutions and uncertainties caused by the above single research methods.

In this study, we have selected the continuous 1.2 km thick Cretaceous strata from a river section exposed at the southwestern corner of the Sichuan Basin (SWCSB) around the village of “Feixianguan” (completely unrelated to the Lower Triassic “Feixianguan” Formation found elsewhere in the Sichuan Basin) is analyzed here in this multi-proxy provenance study (Figure 2). This

section was magneto-stratigraphically dated in detail (Zhuang et al., 1988; Otofujii et al., 1990; Enkin et al., 1991), and predecessors have accumulated abundant sedimentology, paleontological and elemental geochemistry data near it (Li, 1979; Wei, 1979; Li, 1982; Ye, 1983; Gou, 1998; Li, 1988; Yang et al., 2010; Li et al., 2013). For our study we combined fieldwork and modal framework grain composition of the sandstones, conglomerate clasts composition, heavy mineral analysis, and detrital garnet geochemistry from the Tianmashan, Jiaguan, and Guankou Formations to characterize the lithologies in the source areas

of the Sichuan Basin though Cretaceous period. These data, in combination with stratigraphic records and tectonothermal events evidence, provide important constraints on the early uplift and denudation history of the eastern margin of the Tibetan Plateau.

2 Geology setting and potential provenance

The hinterland of the southwest corner of the Sichuan Basin comprises, from west to east, potential source rocks derived from the following tectonic units: Songpan-Ganzi fold belt, Yidun terrane, and Longmenshan orogenic belt. Here we summarize the age, lithology, and tectonic association of potential sources for recent work of the detrital zircon geochronology and heavy mineral analysis from the Cretaceous basin fill.

2.1 Songpan Ganzi fold belt (SPGZ)

The West of the Longmenshan orogenic belt, the triangular-shaped Songpan-Ganzi turbidite fold belt (Figure 1), which represents a Paleo-Tethyan accretionary complex (Chen et al., 1995), is dominated by a thick succession of Middle-Upper Triassic flysch turbidites that settled mainly during Ladinian through Norain (230 Ma–203 Ma) (Huang and Chen, 1987; Brugier et al., 1997; Weislogel et al., 2006; Enkelmann et al., 2007; Zhang et al., 2008; Zhang et al., 2012). Moreover, the only deep oil exploratory well HC1 of 7,012.4 m located in the area shows at least six times tectonic repetitions, resulting in more than ~46% thickening of the Triassic sequence (Liu et al., 2013b). It indicates that the true thickness of the Songpan-Ganzi Triassic flysch is not 10 km–15 km as previously assumed (BGMRSP, 1991), but not more than 3 km–5 km (Liu et al., 2013b). From the end of the Late Triassic to the Early Jurassic, most flysches were intensely folded and uplifted (Burchfiel et al., 1995), which is associated with the amalgamation involving the Qiangtang block and accompanied by synchronous east-directed emplacement of the Longmenshan orogenic belt (Chen et al., 1995). The Songpan-Ganzi Triassic flysch has a multi-provenance origin with peak zircon ages of 265 Ma, 440 Ma, 740 Ma, 1,860, and ca.2,450 Ma (Weislogel et al., 2006, 2010; Enkelmann et al., 2007; Deng et al., 2008; Ding et al., 2013; Zhang et al., 2014; Tang et al., 2017; Jian et al., 2019; Gong et al., 2021), and experienced low-to medium-grade greenschist facies metamorphism during the Late Triassic–Early Jurassic (BGMRSP, 1991; Dirks et al., 1994; Brugier et al., 1997; Huang et al., 2003; Wilson et al., 2006; Roger et al., 2010). In contrast, the underlying upper Sinian–Palaeozoic sequences, predominantly composed of carbonates, experienced higher-grade, medium-pressure metamorphism (Huang et al., 2003). Heavy mineral assemblages in the Triassic flysch contain abundant zircon, apatite, garnet, leucosene, haematite-limonite, tourmaline, epidote, and rutile (Zhang et al., 2008; Yan et al., 2014; Tang et al., 2017). The geochemical analysis of clastic garnet shows that the type of garnet is mainly Bi (70%) type and Type A (18%) (Zhang et al., 2008; Yan et al., 2014). During the Mesozoic, large amounts of granodiorite to monzonite with ages of 228 Ma–185 Ma were emplaced in the flysch turbidites (Roger et al., 2010; Ding et al., 2013; Zhang et al., 2014).

2.2 Yidun terrane

The Yidun terrane is located to the southwest of the SPGZ, bounded by the Jinsha and Ganzi-Litang suture zone in the south and north respectively (Figure 1). From west to east, it includes the Precambrian–Paleozoic Zhongza massif, Middle Triassic–Early Jurassic eastern Yidun felsic plutons, and middle Cretaceous West Yidun felsic plutons (120 Ma) (Jian et al., 2019). The Zhongza massif is composed of Neoproterozoic basement rocks consisting of granitic gneisses and metavolcanic rocks (Bureau of Geology and Mineral Resources of Sichuan Province (BGMRSP, 1991) and a cover sequence of Paleozoic greenschist facies metasedimentary rocks, shallow-to deep-marine carbonates, and clastic rocks intercalated with sporadic mafic volcanic rocks (BGMRSP, 1991; Chang, 2000). The eastern Yidun Terrane includes widespread exposure of the Triassic Yidun Group flysch that is intruded by large Late Triassic dioritic-granitic plutons (230 Ma–210 Ma) (Reid et al., 2007; Weislogel, 2008; Jackson et al., 2018a; Jackson et al., 2018b). Detrital zircon ages from the Yidun Group in the northern part of the Yidun terrane show prominent bimodal characteristics of 400 Ma–480 Ma and 880 Ma–980 Ma, with a small number of ages of 2,450 Ma–2,500 Ma (Wang et al., 2013). The detrital zircons from the southern Yidun Group are mainly ~220 Ma–240 Ma, ~400 Ma–480 Ma, ~720 Ma–1,000 Ma, ~1,700 Ma–1,900 Ma, and ~2,400 Ma–2,500 Ma (Ding et al., 2013; Wang et al., 2013; Liu et al., 2021).

2.3 Longmenshan orogenic belt (LMS)

The Longmenshan orogenic belt, separating the Songpan-Ganzi turbidite fold belt to the west from the Western Sichuan foreland basin to the east (Figure 1), evolved into an intracontinental transpressional orogen in the Late Triassic (Burchfiel et al., 1995; Chen et al., 1995; Worley and Wilson, 1996). It is NE-SW trending, approximately 500 km long by 30 km–50 km wide (Lin et al., 1996; Jia et al., 2006; Lin, 2008). This belt is characterized by numerous large-scale nappes separated by several NW-dipping thrusts (Jia et al., 2006), in which deformed Paleozoic passive margin carbonate rocks of South China Block and Precambrian crystalline basement massifs are involved (Ministry of Geology and Mineral Resources, 1991; Burchfiel et al., 1995). The massifs consist of high-grade metamorphic quartzofeldspathic gneisses and associated granitoids with an age of 699 Ma–864 Ma (Zhou et al., 2002a; Zhou et al., 2002b; Zhou et al., 2006a; Druschke et al., 2006; Sun et al., 2007; Zhao and Zhou, 2007; Yan et al., 2008). The passive margin sequence itself consists primarily of shallow water marine rocks of Neoproterozoic (Sinian) to Permian age (BGMRSP, 1991; Guo et al., 1996; Yan et al., 2008). Directly northwest of Longmenshan, Paleozoic metasedimentary units of the Maoxian Group are exposed within the Maoxian-Wenchuan shear zone (BGMRSP, 1991; Worley and Wilson, 1996; Yan et al., 2011). The detrital zircons of Paleozoic sedimentary rocks in the Longmenshan orogenic belt are aged 490 Ma–670 Ma, 730 Ma–850 Ma, 900 Ma–1,000 Ma, and 2,450 Ma–2,550 Ma. The peak ages were ~554 Ma, ~800 Ma, ~940 Ma, and ~2,500 Ma, respectively (Duan et al., 2011; Chen et al., 2016, 2018). Heavy mineral assemblages in the Longmenshan region contain abundant garnet, sillimanite, staurolite, and kyanite (BGMRSP, 1991; Worley and Wilson, 1996). Airaghi et al. (2017b)

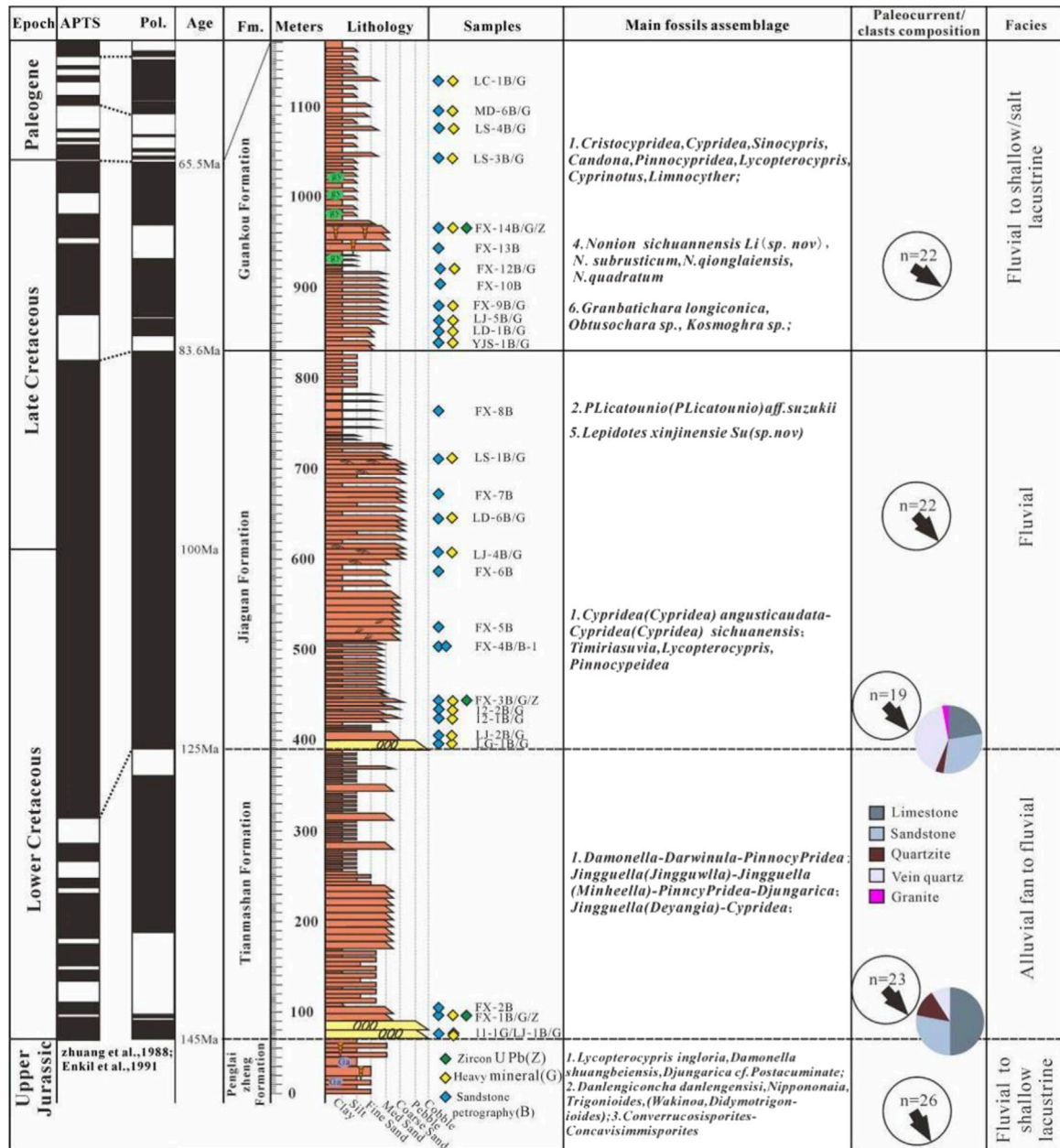


FIGURE 3 Comprehensive stratigraphic column of the Cretaceous in the SW Sichuan Basin, indicating the position of analyzed samples, and upward compositional variations in conglomerates. The geomagnetic polarity time scale (GPTS) is from Harland et al. (1982), and the observed polarity data are from Zhuang et al. (1988), Enkin et al. (1991). Fossil data are compiled from BGMRSP (1991), Wei (1979), Ye (1983), Chen (1983), Su (1983), Li (1987), Gou (1998) and Wang et al. (2006). 1 Ostracoda; 2 Lamellibranchia; 3 Pollen; 4 Foraminifera; 5 Fish; 6 Charophyte.

showed that there was obvious uplift and denudation in the lower Cretaceous (137 Ma) of Longmenshan orogenic belt.

2.4 Cretaceous sedimentary strata in Western Sichuan Basin

Mesozoic sedimentary basins are widespread along the eastern Tibetan Plateau. As the largest Mesozoic sedimentary basin of the Upper Yangtze plate (Figure 1), the Sichuan Basin is located to the east of the Tibetan Plateau with a total area of 18×10^4 km² (Tong, 1992). It

is a multi-stage, superimposed basin characterized by three main basin evolution processes: marine carbonate platform (Eidacaran to Late Triassic), Indosinian-Yanshanian orogeny foreland basin (Late Triassic to Late Cretaceous), and uplift and tectonic modification (Late Cretaceous to Quaternary) (Chen et al., 1995; Guo et al., 1996; Liu et al., 2018; Deng et al., 2013a, b; Li Z W et al., 2012; Li J Z et al., 2009; Li W et al., 2009; Shen et al., 2009; Liu et al., 2008; Richardson et al., 2008). Since the Late Triassic, the Sichuan Basin had become a typical continental sedimentary basin (Liu, 1993; Li Y et al., 2003).

The exposed Cretaceous terrestrial sediments sequence consists entirely of non-marine synorogenic deposits, including lacustrine,

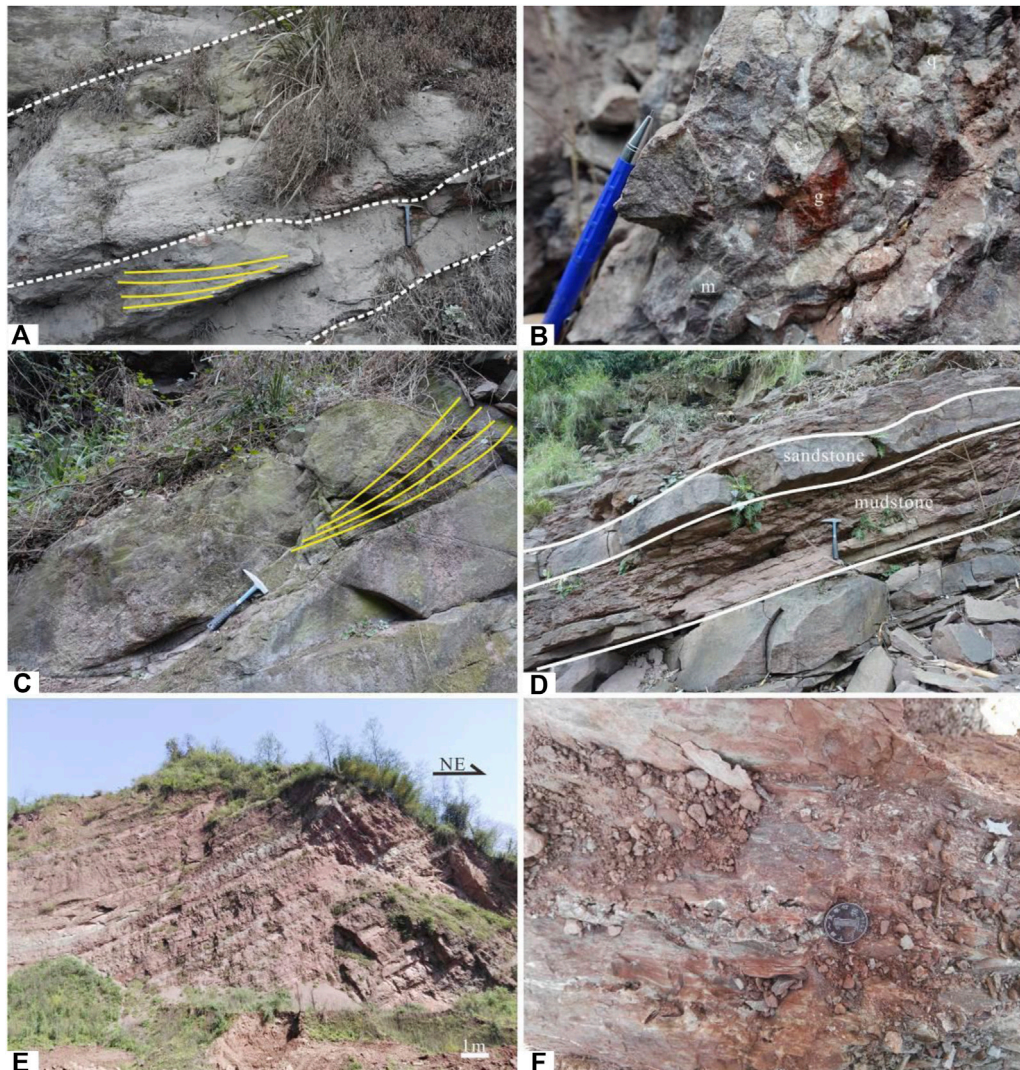


FIGURE 4

Typical outcrops photographs from the Feixianguan section. (A) Channel bottom scour surface and conglomerate in the Tianmashan Formation. (B) Basal conglomerate in the Jiaguan Formation. (C) Massive medium-coarse sandstone with low-angle oblique bedding, Jiaguan Formation. (D) Interbedded sandstone and mudstone at the top of the Jiaguan Formation. (E) Brownish red lacustrine mudstone of Guankou Formation. (F) Brownish red mudstone with dissolved pores in the Guankou Formation. c-Limestone clast. m- Metasandstone clast. g- Granite clast.

alluvial fan and fluvial sandstone and conglomerate, siltstone, and mudstone [Bureau of Geology and Mineral Resources of Sichuan Province (BGMRSP), 1991]. Cretaceous strata exist only in the southeast, west, and northwest of the Sichuan Basin, with the central basin dominated by Jurassic red beds (Bureau of Geology and Mineral Resources of Sichuan Province (Compiling Group of Continental Mesozoic Stratigraphy and Palaeontology in Sichuan Basin of China, 1982; Zhuang et al., 1988; BGMRSP, 1991).

In the study area (Figure 2), the Cretaceous strata are composed of (from oldest to youngest) the Tianmashan (K_1t), Jiaguan (K_{1-2j}), and Guankou (K_2g) Formations (Figure 3). These strata locally exceed 3,000 m in total thickness in the Southwest corner of the Sichuan Basin (Figures 1, 2). Sedimentary rocks interpreted to have been deposited in the foreland basin thin eastward toward the interior of the Sichuan Basin. This Cretaceous succession in the southwestern corner of the Sichuan Basin is mainly composed of brown red sandstone

interbedded with red mudstone and conglomerate, which exhibit decreasing compositional and textural maturity with time (BGMRSP, 1991; SBGMR, 1997; Gou, 1998).

The sedimentary age of the Cretaceous foreland deposits is well constrained by magnetostratigraphic and fossil data (Wei, 1979; Su, 1983; Li, 1987; Ye, 1983; Chen, 1983; Zhuang et al., 1988; BGMRSP, 1991; Gou, 1998; Wang et al., 2006) (Figure 3). Paleomagnetic and paleontological data show that the depositional ages of Tianmashan, Jiaguan, and Guanguou Formations are, in turn, early Cretaceous Berriasian-Barremian, middle Cretaceous Aptian-Santonian and late Cretaceous Campanian-Maastrichtian stage (Figure 3) (Zhuang et al., 1988; Li and Ji, 1993; Gou, 1998).

The Early Cretaceous Tianmashan Formation is 350 m thick and parallel unconformably overlies the Upper Jurassic Penglaizheng Formation (Chengdu Institute of Geology and Mineral Resources (CGMR), 1979; BGMRSP, 1991; Wang et al., 2006) (Figure 3). It is composed of brown-red quartz-lithic sandstone interbedded with

mudstone and conglomerate lenses, with thick-bedded massive conglomerate at the base (Figure 4A). The depositional environment is interpreted as alluvial fan and fluvial deposits (CGMR, 1979; BGMRS, 1991; Gou, 1998; Li et al., 2016b). The conglomerate bed is commonly present in the basal portion of the Tianmashan Formation, approximately 10 m thick and consists of massive, light brown-red, matrix to clast supported, calcium cemented. The matrix is sandy to silty and normally is purple to reddish-purple in color. The clasts are ranging from 2 mm to 15 mm in size (average 5 mm), and are mainly composed of sub-rounded to rounded limestone, quartz sandstone, quartzite, and vein quartz. They often show fining-upward sequence and occasional gravel shingle imbricate structures, and we interpret this conglomerate bed as a lag deposit of a meandering river. Non-marine Cretaceous ostracod assemblages of the Tianmashan Formation are characterized by *Jingguella*—*Pinnocypridea*—*Damonella*—*Minheella* (Wei, 1979; Ye, 1983; Chen, 1983; Li, 1987; Wang et al., 2006), combined with paleomagnetic data (Zhuang et al., 1988), the sedimentary age corresponding to ca. 145 Ma–125 Ma (Figure 3).

The ~420-m-thick Jiaguan Formation was parallel unconformity above the Tianmashan Formation (Figure 3) and consists of a fining-upwards unit of red, conglomerate, feldspar-quartz sandstone, siltstone, and mudstone (Figures 4C, D). Whereas the Jiaguan Formation corresponds to a braided river environment (SBGMR, 1993; Gou, 1998; Li J. et al., 2016). Non-marine Cretaceous ostracod assemblages of the Jiaguan Formation are characterized by *Cypridea*—*Monosulcocypris* (Wei, 1979; Ye, 1983; Chen, 1983; Li, 1987; Wang et al., 2006), combined with paleomagnetic data (Zhuang et al., 1988), corresponding to ca. 125 Ma–83.6 Ma (Figure 3). The conglomerate beds are commonly present at the bottom of the Jiaguan Formation. Their composition and texture are varied. Pebbles and cobbles are generally rounded to subangular and are composed of metamorphic rocks and volcanic rocks, quartzite, vein quartz, sandstone, and carbonate clasts (Figure 4B).

The Upper Cretaceous Guankou Formation overlies the Jiaguan Formation and has an age of ca. 83.6 Ma–66 Ma (Zhuang et al., 1988), with non-marine Cretaceous ostracod assemblages characterized by *Cristocypridea*—*Sinocypris* (*Quadracypris*)—*Lunicypris* (Wei, 1979; Ye, 1983; Chen, 1983; Li, 1983; Li, 1987; Wang et al., 2006). This formation consists predominantly of 800 m brown-red mudstone with unequal siltstone and comparatively thick marlstone, fine conglomerates, gypsums, and halite (BGMRS, 1991; Wang et al., 2006) (Figures 4E, F), which were deposited in fluvial to closed lacustrine sedimentary environment (BGMRS, 1991; SBGMR, 1993; Gou, 1998) (Figure 3).

3 Sampling and methodology

A combination of paleocurrent data, sandstone modal framework point-count data, conglomerate clast compositions, heavy mineral analysis, detrital zircon U-Pb age dating, and single grain detrital garnet major element geochemistry analysis was performed to determine the provenance of the Cretaceous sediments in the southwest corner of the Sichuan Basin, and the tectonic evolution of the source area. Analytical methods, including separation, identification, and quantification techniques, are described as flowing:

3.1 Paleocurrent

To determine the paleotransport directions, paleocurrent indicators (trough-cross, conglomerate clast imbrications, and oblique bedding) were measured wherever possible in the stratigraphic sections to infer the input direction of the detrital material. A total number of 112 directional data were collected from the Late Jurassic Penglaizheng to Late Cretaceous Guankou Formation (Figure 3). All the paleocurrent data were corrected to horizontal by standard stereonet techniques (DeCelles et al., 1983), and the corrected data are then plus or minus 180° (Wu et al., 2012), and plotted the average value represented by a black arrow (Figure 3).

3.2 Gravel and sandstone petrography

The lithology, size, sorting and roundness of conglomerate clasts were assessed by conducting *in situ* clast counts at bottom of Tianmashan and Jiaguan Formations, respectively (Figure 3). Locations of the clast counts and various lithological types at each site are shown in the stratigraphic column (Figure 3). In addition, we collected clasts composition data from 20 locations on the western margin of the Sichuan Basin from published literature to compare regional provenance changes in clast types and identify specific sediment sources (Figure 5).

Sandstone framework compositions were collected from 27 standard petrographic thin sections of samples obtained from Cretaceous sandstones (Figures 3, 6). These medium-grained sandstone samples were systematically collected to represent the variations in stratigraphy, lithology, and composition through the Tianmashan, Jiaguan, and Guankou Formations along the log of the SW of the Sichuan Foreland Basin. The logged section and the position of selected samples for different analyses are given in the stratigraphic column (Figures 3, 6). Thin sections were stained for potassium and calcium feldspar, and at least 300 relevant grains of quartz, feldspar, and lithic rock fragments per thin section were counted according to the Gazzi-Dickinson method to reduce the influence of grain size (Dickinson, 1970; Dickinson and Suczek, 1979; Dickinson et al., 1983; Ingersoll et al., 1984). This allows us to examine the detrital framework and understand the composition of sandstones within the Cretaceous strata, which ultimately provides additional information on the composition of source rocks from which the sediment was derived (e.g., Dickinson and Suczek, 1979; Dickinson et al., 1983; Ingersoll et al., 1984). Provenance data from the light mineral assemblage is displayed on the QFL (quartz–feldspar–lithics) and QmFLt (quartz monocrystalline–feldspar–lithic total) diagrams to indicate possible derivation from “continental block”, “recycled orogen” or “magmatic arc” settings (Dickinson et al., 1983). Recent studies have highlighted issues with over-simplified interpretation of these plots when applied in tropical settings (van Hattum et al., 2006; Garzanti et al., 2007; Smyth et al., 2008; Sevastjanova et al., 2012). Therefore, the two triangular diagrams are used to show the composition differences between different Formations without much discussion about the tectonic background of the potential source (Zimmermann and Hall, 2016).

Textural categories from 1 to 4 were assigned for sorting and roundness of grains (Zimmermann and Hall, 2016, 2019; Löwen

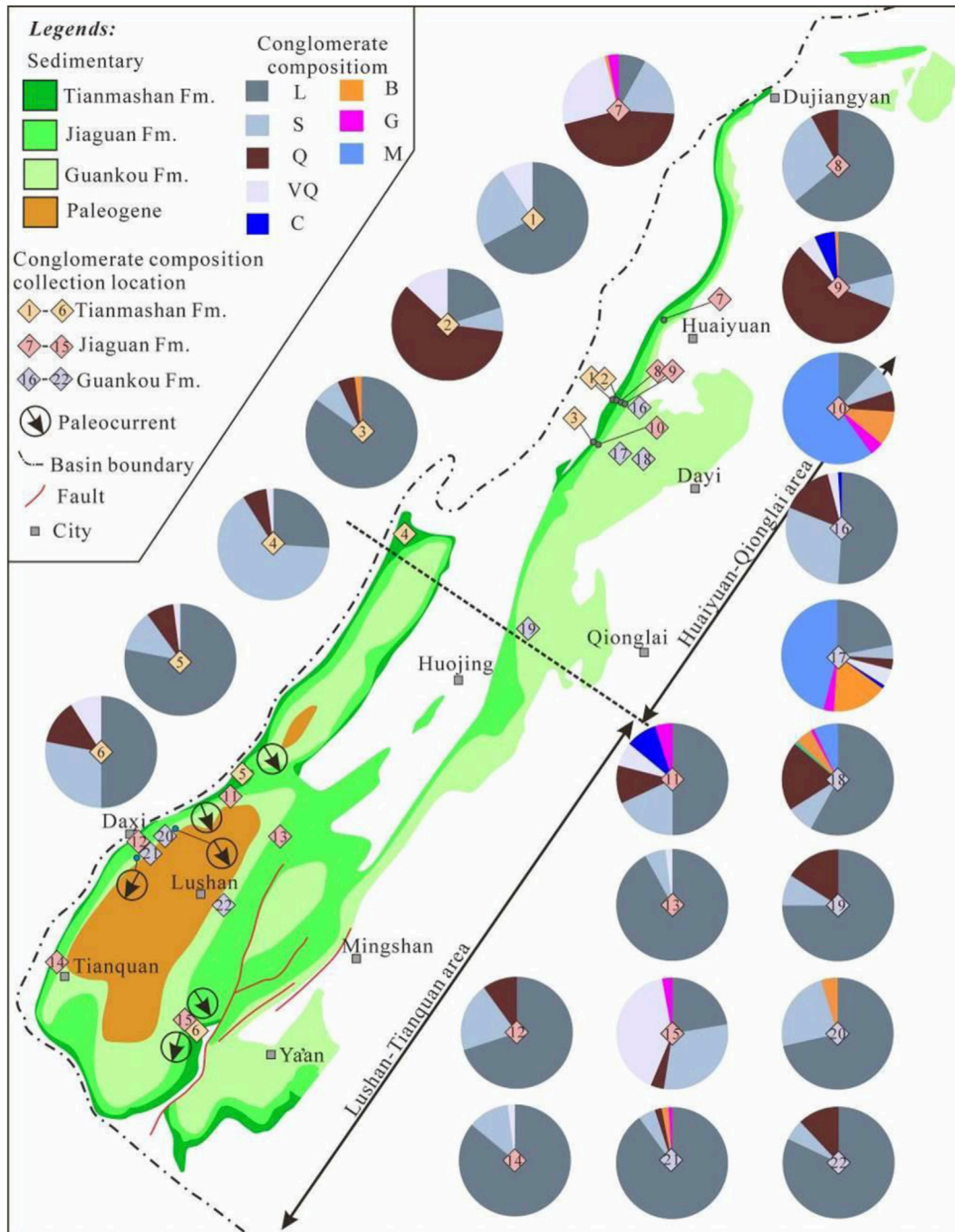
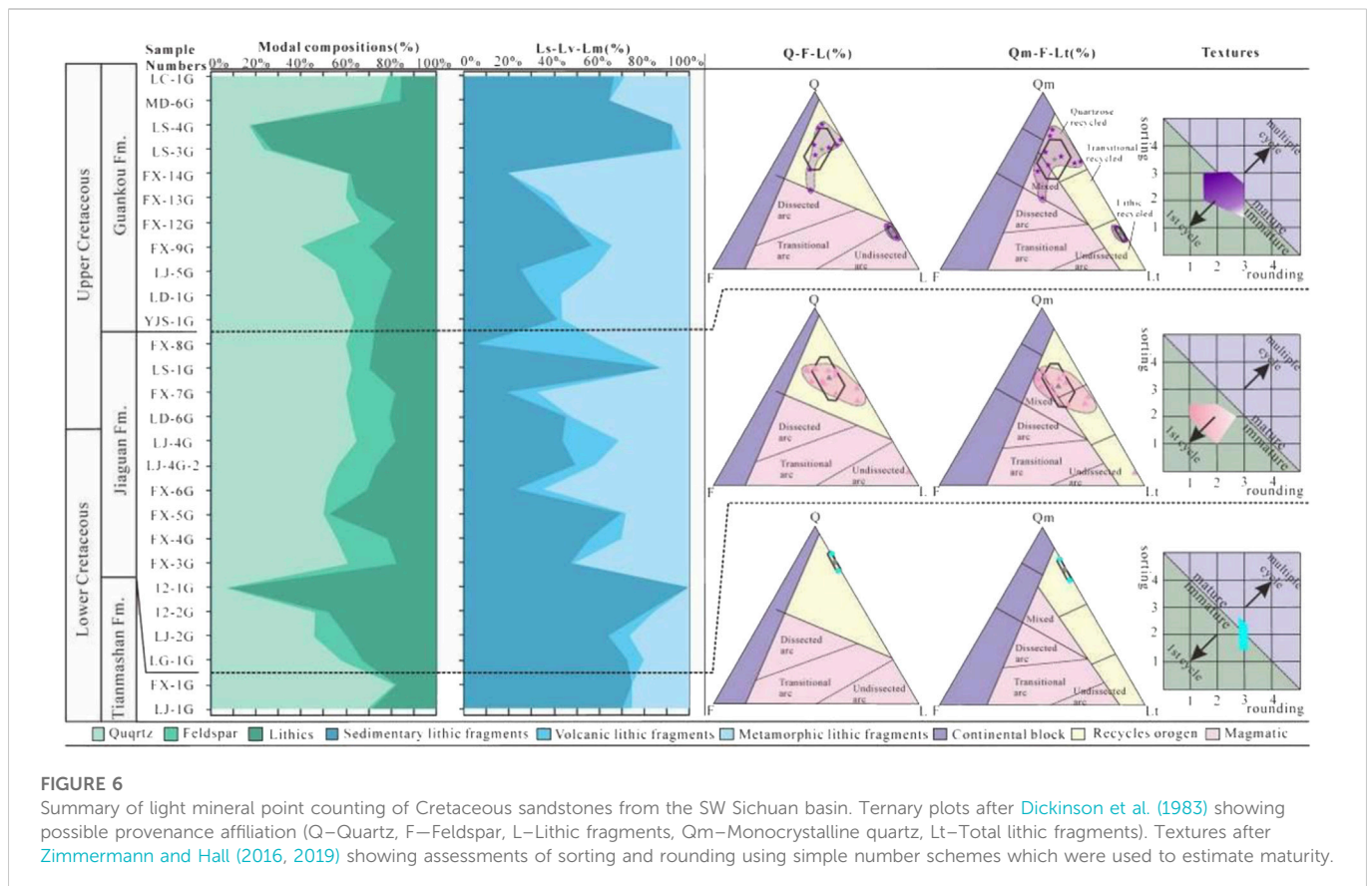


FIGURE 5 The pie charts showing clasts composition of conglomerate from the southwest corner of Sichuan Basin. Clast types in the Cretaceous sandstones: L-limestone, S-sandstone, Q-quartzite, VQ-vein quartz, C-chert, B-basalt, G-granite, M-metamorphic. Clasts composition data from Chengdu Institute of Geology and Mineral Resources (CGMR). (1979), Zeng et al. (2004), Ji and Li, 1995, Li and Ji (1993), Gou (2001), and this study.

et al., 2018). Sorting categories are 1) poorly sorted, 2) moderately sorted, 3) well sorted, and 4) very well sorted. Rounding categories are 1) angular, 2) sub-angular, 3) subrounded, and 4) rounded. Typical examples of Cretaceous rocks are shown in Figure 3. The collection of conglomerate compositional data was conducted at two outcrop localities, they come from the bottom of the Tianmashan Formation and the Jiaguan Formation, respectively (Figure 3).

3.3 Heavy mineral assemblages

There were 21 heavy mineral separates analyzed, comprising three samples from the Tianmashan Formation sandstones, eight samples from the Jiaguan Sandstone, and 10 samples from the Guankou, respectively (Figure 3). To make sure the samples were representative, each sandstone sample is fresh fine-to coarse-grained with an average grain size between 0.2 mm–2 mm,



weighing at least ~1.5 kg–2 kg. Heavy mineral separation was disaggregated using a ceramic mortar and pestle, and wet-sieved into four grain-size categories: > 1 mm, 0.25 mm–1 mm, 0.0625 mm–0.25 mm, and < 0.0625 mm, and the 0.0625 mm–0.25 mm sand fraction was then processed by density separation using sodium polytungstate with a density of 2.89 g cm⁻³ (Morton, 1985; Mange and Maurer, 1992; Morton & Hallsworth 1994). 300 heavy mineral grains per sample were classified.

Heavy mineral analysis is one of the most sensitive and widely used methods to determine possible provenance areas of sandstones (e.g., Mange and Maurer, 1992; Morton and Hallsworth, 1994, 1999). Hence, they often do not reflect the original composition of the source area (Morton and Hallsworth, 1994). Common ultra-stable heavy minerals were categorized into groups corresponding to their most likely protoliths, based on suggested source rocks (Feo-Codecido, 1956; Mange, 2002; Nichols, 2009). Based on the types of heavy minerals isolated from the samples and the background information of potential provenance, common heavy minerals were grouped by their most likely protoliths, based on suggested source rock associations (Mange, 2002; Nichols, 2009; Zimmermann and Hall, 2016, 2019) zircon, tourmaline, anatase, monazite, and apatite are considered to indicate acid igneous (granitic) sources. Magnetite, ilmenite, and chromium spinel represent basic igneous and ultrabasic sources. Rutile and garnet are interpreted to indicate metamorphic sources, mainly of continental character. Other minerals, such as barite, haematite-limonite, and leucoxene are thought to be sedimentary rock sources.

The provenance-sensitive heavy mineral ratios ATi (apatite: tourmaline index), GZi (garnet: zircon index), RuZi (rutile: zircon

index), MZi (monazite: zircon index) and CZi (chrome spinel: zircon index) were determined following Morton and Hallsworth (1994) and Morton et al. (2005). In addition, the ZTR index (zircon, tourmaline, rutile) was calculated as defined by Hubert (1962) (Figure 8).

3.4 Detrital garnet geochemistry

Garnet is a very common heavy mineral that occurs in a wide range of metamorphic and igneous rocks and is relatively stable during sedimentary transport and burial diagenetic conditions (Wright, 1938; Morton, 1985; Deer et al., 1992). Its comparatively wide range of major and trace element composition is primarily controlled by host rock composition and reflects changes in pressure and temperature conditions during mineral growth as well (Mange and Morton, 2007; Krippner et al., 2014). Therefore, the mineral chemistry of detrital garnet is widely used as a provenance indicator in studies of sedimentary rocks (Mange and Morton, 2007; Krippner et al., 2014, 2015, 2016; Huang et al., 2019b).

In order to characterize the detrital garnets in the Western Sichuan foreland, three samples were taken from the Tianmashan, Jiaguan, and Guankou Formation, fine-to medium-grained fluvial sandstones, respectively. Garnet major element geochemistry analysis was performed with a JEOL JXA8230 RL EMP equipped with five wavelength dispersive spectrometers at the Sample Solution, Wuhan, Hebei Province. Measuring conditions for garnet include a beam current of 20 nA and an accelerating voltage of 15 kV. The counting times per spot were 15 s for Si, Mg, Ca, Fe, and Al, and 30 s for Ti, Cr, and Mn. Garnet assemblages have been compared by

determining the relative abundances of garnet types A (low-Ca, high-Mg), Bi (low-Mg, Ca < 10%), Bii (low-Mg, Ca > 10%), and C (high-Mg, high-Ca), as defined by [Mange and Morton \(2007\)](#). Previous studies have shown that garnets from felsic crystalline rocks (e.g., intermediate–acidic igneous rocks and metapelites) often have similar major element composition ([Mange and Morton, 2007](#)), while there are significant differences in trace elements, which can be effectively used to distinguish garnets from medium-acidic igneous rocks and different metapelite rocks ([Lenaza et al., 2018](#); [Hong et al., 2020a, 2020b](#)).

It is possible to compare potential source compositions to the detrital ones because the potential source rocks were already narrowed down to particular regions based on other provenance proxies and because many of these rocks are still preserved in the western provenance of the basin today. For comparison we used data from published source rocks data from different units including Triassic flysch from the southern Songpan-Ganzi ([Zhang et al., 2008](#)), Early and Middle Triassic sandstones in the West Qinling ([Yan et al., 2014](#)), Triassic granite within the Ganzi-Litang suture zone ([Li et al., 2017](#)), Metamorphic crystalline basement of Yidun terrane ([Tian et al., 2018](#)), Metamorphic massifs in Longmenshan orogenic belt ([He et al., 1988](#)), Metamorphic rocks in Danba area of the southeast corner of Tibetan Plateau ([Huang et al., 2003](#); [Billerot et al., 2017](#)), and garnet from modern river sands in the upper Reaches of the Yangtze River (Wang et al., 2018).

3.5 Detrital zircon U-Pb age

Three middle-coarse sandstone samples (FX-1G, from Tianmashan Formation; FX-3G, from Jiaguan Formation, and FX-14G from Guankou Formation) were used for zircon U-Pb dating analysis. At least 250 zircon grains were randomly selected and mounted in epoxy resin and polished to nearly half their original width to expose the internal structures. The internal texture of the zircons was observed with transmitted and reflected light micrographs and cathodoluminescence (CL) images. U–Pb dating was generated from detrital zircons using laser-ablation inductively coupled plasma mass spectroscopy (LA–ICP–MS) at the State Key Laboratory of Continental Dynamics, Department of Geology, Northwest University, Xi'an, China, following a procedure similar to that reported by [Yuan et al. \(2007\)](#). Eighty detrital zircons from each sample were analyzed with a spot size of 32 μm using an Agilent 7,500a ICP–MS coupled to a Lambda Physik Geolas 200 M excimer laser ablation system (193 nm). U–Th–Pb isotopic data were simultaneously acquired on the same spot.

Isotopic ratios and element concentrations of zircon grains were calculated by GLITTER (ver. 4.0, Macquarie University), and were corrected for both instrumental mass bias and depth-dependent elemental and isotopic fractionation using Harvard zircon 91,500 as an external standard with a recommended $^{206}\text{Pb}/^{238}\text{U}$ age of $1,065.4 \text{ Ma} \pm 0.6 \text{ Ma}$ ([Wiedenbeck et al., 2004](#)). Concordia ages and diagrams were obtained using Isoplot/Ex (ver. 3.0; [Ludwig, 2003](#)). Common lead was corrected by the LA–ICP–MS common lead correction (ver. 3.15) method, following [Andersen \(2002\)](#). Interpreted ages were based on $^{206}\text{Pb}/^{238}\text{U}$ for younger than 1,000 Ma grains and on $^{206}\text{Pb}/^{207}\text{Pb}$ for older than 1,000 Ma grains. Only zircon ages with 90%–110% concordance were used to estimate percentages and build a probability plot of each sample, and considered in the

following discussions. The analytical data are reported in Supplementary data (See [Supplementary Material](#) for details).

We also collected detrital zircon geochronological data of four published samples to compare with the new data ([Figure 2](#)), including sample G124 (Jiaguan Formation), G136 (Jiaguan Formation), G130 (Guankou Formation), and G178 (Guankou Formation) ([Li et al., 2018](#)).

4 Results

4.1 Paleocurrent

To reconstruct the organization of flow direction during the foreland basin evolution in the study area, 86 new palaeocurrent data (23 in Tianmashan Formation, 41 in Jiaguan Formation, 22 in Guankou Formation) were measured from the gravel slant plane and the direction of inclination of the oblique bedding and combined with 124 palaeocurrent measurements previously published from the Jiaguan and Guankou Formations ([Li and Ji, 1993](#); [SBGMR, 1993](#)). Measurements indicate a clear SE-directed transport direction ([Figure 3](#)). There is no significant change that occurs in paleocurrent patterns. Paleocurrent data show that from the Early Cretaceous Tianmashan Formation to the Late Cretaceous Guankou Formation in the southwestern Sichuan Basin, the palaeoflow pattern was inherited, and the main body was SE 110°C – 220°C with an average of 130°C ([Figures 3, 5](#)). It is suggested that the source area of sediments is located at the West and Northwest of the basin from Longmenshan orogenic belt and the Songpan-Ganzi fold belt.

4.2 Gravel and sandstone petrography

4.2.1 Conglomerate clasts composition

In the Feixianguan section, clasts at the bottom of the Tianmashan Formation consist of gray-white carbonate (85%), quartz sandstone (8%), quartzite (5%), and a little volcanic rock (2%) ([Figures 3, 5](#)). In contrast, the conglomerate clasts composition at the bottom of the Jiaguan Formation changed significantly and is mainly composed of subrounded vein quartz (42%), followed by sub-angular sandstone (31%), limestone (23%), and minor amounts of quartzite (4%) and granite (3%). There is an upsection increase in sandstone and vein quartz clast, while decrease significantly in carbonate clasts ([Figure 3](#)).

Regional stratigraphy and sedimentology studies show that the conglomerates in each formation mainly developed in the front of the Longmenshan orogenic belt in the western margin of the Sichuan Basin ([SBGMR, 1993](#); [Gou, 1998](#)). In order to better understand the provenance information in the region, we collected the conglomerate clasts composition data of the front edge of the Longmenshan orogenic belt from the published literature ([CGMR, 1979](#); [Zeng et al., 2004](#); [Li and Ji, 1993](#); [SGMB, 1993](#); [Ji and Li, 1995](#); [Gou, 2001](#)) and discussed together with our new statistical data. Spatially, the conglomerates can be divided into two small ranges: Huaiyuan–Qionglai area and Lushan–Tianquan area ([Figure 5](#)).

At the Dayi–Qionglai area, clasts in the Tianmashan Formation are mainly limestone (26%–85%), sandstone (7%–65%), quartzite (0%–60%), and vein quartz (0%–13%). The average proportions are as follows: limestone, 50%; sandstone, 26%; quartzite, 18%; vein

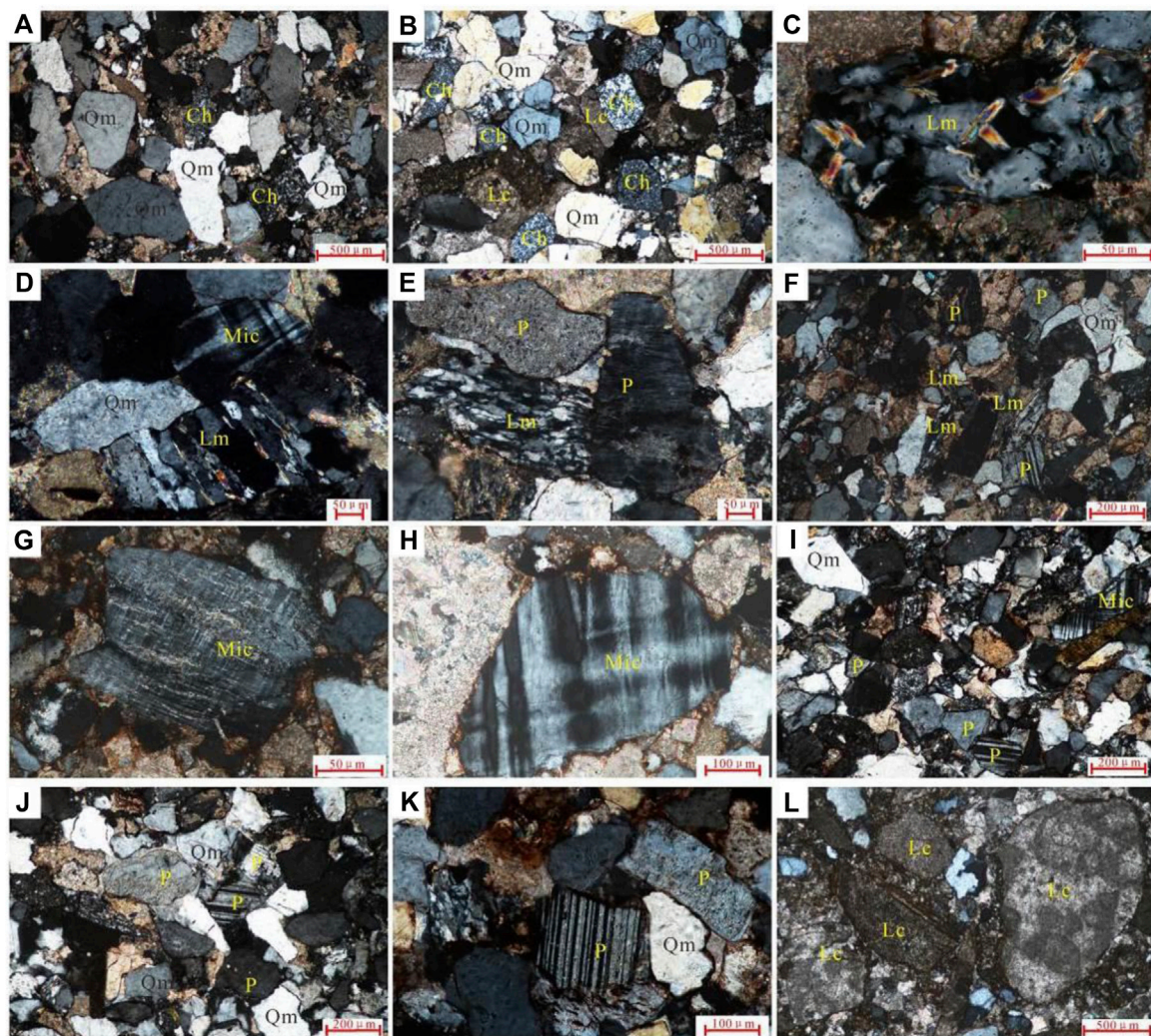


FIGURE 7

Selection of thin section photomicrographs of light minerals (crossed polarized light) in the Tianmashan (A–C), Jiaguan (D–I), and Guankou (J–L) Formations. Qm, monocrystalline quartz; Lm, metamorphic lithic; Lc, carbonate lithic; Ch, chert lithic; Mic, microcline; P, plagioclase.

quartz, 6%. Major clast types in the Jiaguan Formation are quartzite (average 29%), limestone (average 26%), sandstone (average 16%), metamorphic rocks (average 15%), and vein quartz (average 10%). Minor clasts include basalt (average 3%), chert (average 2%), and granite (average 2%). Major clast types in the Guankou Formation are the same as those in the Jiaguan Formation, namely limestone (22%–75%, average 52%), quartzite (3%–20%, average 14%), metamorphic rocks (1%–46%, average 14%), sandstone (4%–30%, average 13%) and basalt (0%–16%, average 5%). The quartz conglomerate is mainly developed near Dayi and is related to the ancient river course, their parent rocks may be the Devonian Pingyipu Formation or the Precambrian basement (SBGMR, 1993; Gou, 2001).

In the Lushan–Tianquan area, major clast types in the three Formations are the same, namely limestone, sandstone, quartzite, and vein quartz. According to the stratigraphic order from Tianmashan to Guankou Formation, the amount of limestone clast increases upsection from an average of 64%–82%, and the amount of sandstone clasts decreases from an average of 20%–12%, and the amount of quartzite clasts decreases from an average of 11%–5%, the

amount of vein quartz increases upsection from an average of 4.5%–11% and then to decreases zero (Figure 5).

The carbonate clasts in Tianmashan Formation are mainly purple micrite, and their parent rock is supposed to be the Triassic Feixianguan Formation. The limestone clasts of the Jiaguan Formation are mainly microcrystalline limestone. The fusulinids and bivalve fossils in the limestone gravel indicate that the source rocks of the clasts were mainly from the Permian-Triassic carbonate rocks (Gou, 2001). The abundant microfossil assemblages (stromatoporoid and brachiopoda) in the Guankou Formation carbonate clasts are similar to reported microfauna from the upper Devonian Yangmaba and Guanwushan Formation (SBGMR, 1993; Li and Ji, 1993; Gou, 2001). In addition, the microfossils of foraminifera and gastropods indicate the some clasts of the Guankou Formation are derived from Permian-early-mid-Triassic Carbonates (Gou, 2001).

4.2.2 Sandstones petrology

Figure 6 shows the results of point counting and textural analysis of sandstones from the southwest corner of the Sichuan Basin. In

general, samples are dominated by quartz, lithic fragments with varying abundances of feldspar. The lithic is mainly sedimentary rock and metamorphic rock fragments. Textural immaturity is indicated by poor sorting and (sub) angular grain shape.

The sandstones of the Tianmashan Formation are medium to coarse-grained, moderately to poorly sorted (1–2), and consist of sub-rounded to rounded grains (3) (Figures 7A, B). Compositions are dominated by quartz (74%–83%), lithic fragments (16%–24%) (Figures 7B, C), and feldspar (1%–2%). Among them chert rock fragments (5%), carbonate rock fragments (7%), and sandstone and metamorphic rocks (1.5%). The unstable lithic fragment grains are normally less than 10%. Quartz contains a small amount of undulating extinction polycrystalline quartz, with monocrystalline quartz accounting for 80%, and polycrystalline quartz for 2%. Carbonate is the dominant cement. Samples studied, commonly show a “Recycled orogen” and “Quartzose recycled” modal composition on the QFL diagram and the QmFLt diagram (Figure 6).

A major petrographic shift occurs across the boundary between the Tianmashan and the Jiaguan Formations in the Mid-Cretaceous. Above this boundary, a marked decrease in structural and compositional maturity is seen (Figure 6). The content of quartz gradually decreases, and the unstable components of feldspar and mica increase. 14 samples from the Cretaceous Jiaguan Formation are fine- to very coarse-grained and moderately to poorly sorted (1–2) and consist of angular to sub-rounded grains (1–3) (Figure 6). Compositions are dominated by monocrystalline quartz (57%) and polycrystalline quartz (4%), with varying content of feldspar (microcline and plagioclase) (6%–22%) and lithic fragments (13%–46%) (Figures 7D–I), except for sample 12-1G. Rock fragments are c. 30% on average of the modal composition and are mostly sedimentary (23%) and metamorphic (7%) grains (Figures 7D–F). Among them, chert accounted for 2%, carbonate rock fragments accounted for 5%, sandstone fragments accounted for 2%, phyllite and quartz schist fragments accounted for 1%, granite fragments accounted for 0.27%, and mica accounted for 5%. The sample 12-1G was mainly carbonate lithic fragments, with only 8% quartz. As shown in Figure 5, the QFL and QmFLt diagrams indicate a “Quartzose recycled orogen” modal composition (Ingersoll and Suczek 1979; Dickinson 1985). On the textures plot (Zimmermann and Hall, 2016, 2019), samples concentration in the immature field (Figure 6).

Sandstones of the upper Cretaceous Guankou Formation are petrographically identical to the lower part. They are fine- to coarse-grained, poorly to moderately sorted (1–2), and consisting of angular to subround grains (1–3) (Figures 7J–L). There are similarities between sand-type detrital components in the Jiaguan Formation and the Guankou Formation (Figure 6), in which monocrystalline quartz (Figure 7J) accounted for 59.8%, polycrystalline quartz accounted for 7%, feldspar (Figure 7K) accounted for 18%, chert accounted for 3%, and carbonate rocks accounted for 6% of rock fragments, 5% of sandstone debris, 1.52% of metamorphic rock fragments, and 1.5% of mica. The lithic fragments comprise dominantly sedimentary rocks and some metamorphic rocks and represent 13%–2% of the rock. Sample LS-3G and LS-4G were mainly carbonate lithic fragments. As shown in the QFL and QmFLt diagrams indicate a “Quartzose recycled orogen” and “Mixed” modal composition (Ingersoll and Suczek 1979; Dickinson 1985). On the textures plot (Zimmermann and Hall, 2016; Zimmermann and Hall, 2019), most of the sample concentration is in the immature field

(Figure 6). Almost all sandstone samples show contains $\geq 60\%$ quartz, possibly due to quartz grains mainly coming from felsic parent rocks. The unsorted sediments of the Jiaguan and Guankou Formations indicate that they were deposited not far from the source by the fluvial process.

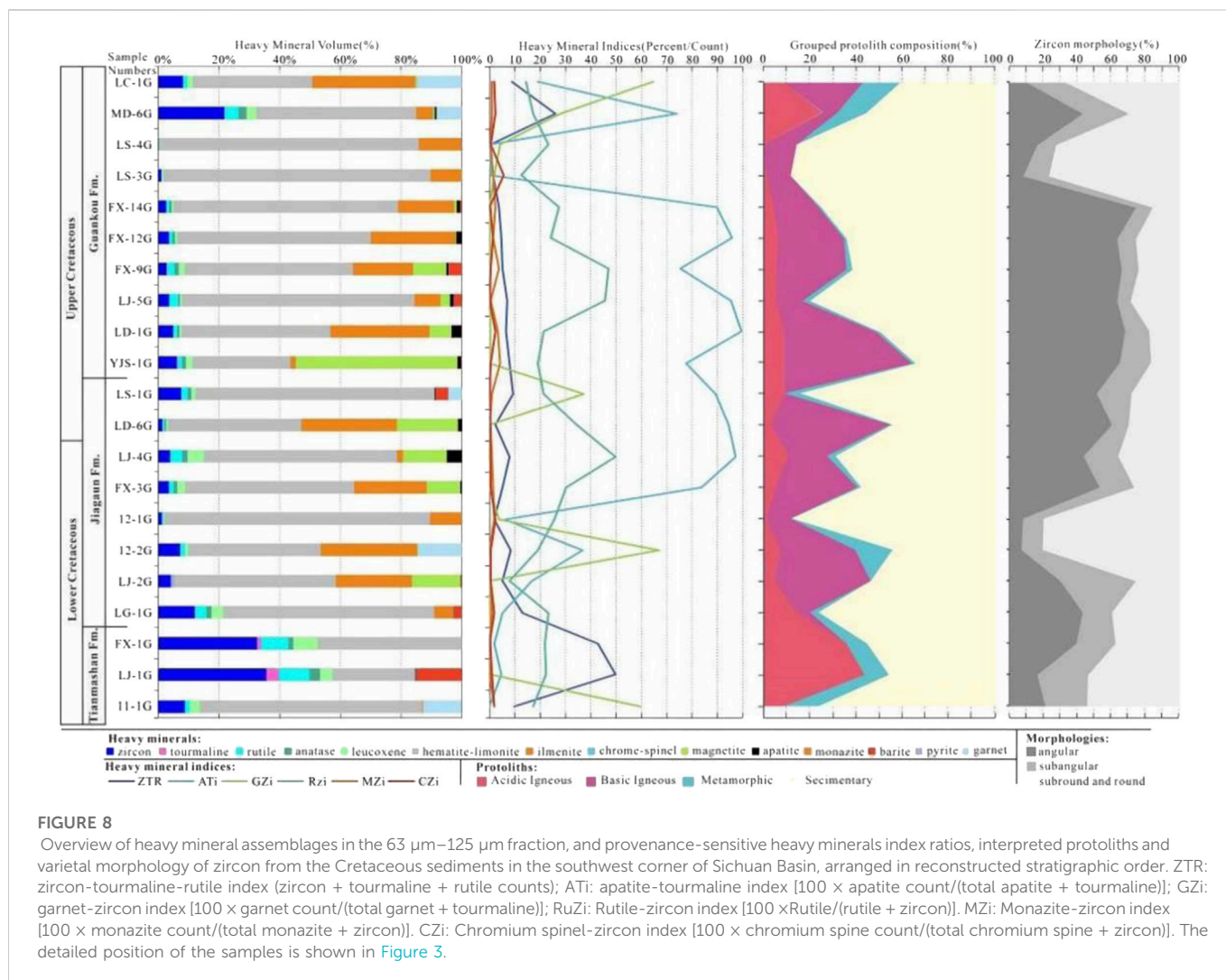
4.3 Heavy mineral assemblages

Figure 8 summarises heavy mineral assemblages, ZTR index, heavy mineral ratios, protoliths, and zircon morphology types of the Lower Cretaceous to Upper Cretaceous sediments. Hematite-limonite and ilmenite are the dominant phase in the Feixianguan section sandstones (average of 72%) and together with zircon and rutile comprises 73%–99% of the heavy mineral fraction. The main heavy minerals detected in the studied samples are haematite–limonite (granular), ilmenite (granular), zircon (euhedral, subhedral, and subrounded), rutile (brown red, columnar, and granular), leucoxene (irregular granular), garnet (pink, irregular granular), apatite (columnar, subhedral, and rounded granular), and barite (granular). However, their relative percentages vary widely, and zircon and apatite exhibit different crystal shapes, indicating the coexistence of two provenances of proximal and distant sources, which might be related to sediment recycling. Other minerals, such as tourmaline (dark brown and columnar), anatase (granular), monazite (granular), and magnetite (granular) are present, either in very low percentages. Chrome spinel (granular) occurs only in a few samples.

Samples 11-1G, LJ-1G, and FX-1G collected from the Early Cretaceous Tianmashan Formation contain the highest abundances of Hematite-limonite (average 46.5%), zircon (average 25.2%), rutile (average 6.9%), leucoxene (average 5%), tourmaline (average 1.8%), and anatase (average 1.7%) and the lowest abundances of ilmenite, apatite, magnetite, and monazite. Sample 11-1G also yields abundant garnet (11.36%), and sample LJ-1G contains abundant barite (15%). These two samples also contain a small amount of chrome-spinel (0.2%). The highest ZTR index value (49.7) is measured in this formation, along with the lowest average ATi (2) and RuZi (20) indices. While intermediate-basic volcanic accessory minerals such as hornblende, epidote, and pyroxene, and aluminosilicate accessory minerals characteristic of medium- to high-grade metamorphic sources, such as andalusite, kyanite, and sillimanite, are absent. Their heavy mineral assemblage reflects their mineralogical maturity and is dominated by the ultra-stable phases with high ZTR value. Less stable accessories are apatite and garnet, and there is a lack of ilmenite and magnetite. The high ZTR index indicates enhanced recycling or chemical weathering.

The Tianmashan Formation in Yaan has a significant acidic igneous (9%–43%) and metamorphic signal (9%–14%) that reflects the abundance of mainly zircon, rutile, and garnet (Figure 8). Sandstones contain on average 59.3% sedimentary rocks and 0.2% basic igneous grains. There is a mixture of angular (39%), subangular (23%), and subround-rounded zircon grains (38%).

In contrast, there is a significant change in provenance in the overlying Jiaguan and Guankou Formations, which have similar heavy mineral assemblage characteristics. Hematite–limonite (average 60%), ilmenite (average 16%), magnetite (average 7.5%), garnet (average 2.2%), apatite (average 1%) and monazite



(average 0.1%) abundances are higher, while zircon (average 4.8%), rutile (average 1.6%), leucoxene (average 1.4%) and tourmaline (average 0.1%) abundances are lower. This stratigraphic interval has the highest mean ATi (56), GZi (11.6), RuZi (26), and MZi (1.32) indices, and the lowest mean ZTR index (6.7). Hematite–limonite and leucoxene represent strong oxidation conditions, are widely distributed in the study area, possibly reflecting the dry oxidation of the climate environment or the decreasing water scale at that time (An et al., 2011; Zhang et al., 2016; Tang et al., 2017), and a very low percentage of zircon, which is interpreted to indicate basic igneous rock sources. The Jiaguan and Guankou Formation sandstones contain a basic igneous (24.5%) and acidic igneous (7.2%) signal indicated by a high percentage of ilmenite, magnetite, and apatite (Figure 8). Zircon grains are a mixture of subround-rounded (38%–44%), subangular (18%), and angular (43%). At the same time, the rutile index also slightly increased (Figure 8). Thus, we infer an increased source input from basic igneous rocks and medium-to high-grade metapelite during the deposition of the Jiaguan and Guankou Formations. Compared with all the samples from the Guankou Formation, the zircon and rutile of the top two samples MD-6G and LC-1G increased, which may be related to the enhanced recycling in the Late Cretaceous (Li et al., 2018).

4.4 Detrital garnet geochemistry

A total of 239 single grains of detrital garnet were analyzed from three samples of the Lower Cretaceous Tianmashan Formation (Sample 11-1G), the Mid-Cretaceous Jiaguan Formation (Samples 12-2G), and the Late Cretaceous Guankou Formation (Sample LC-1G). Results of the garnet single-grain geochemical analysis are shown in the classification scheme after Mange and Morton (2007) (Figure 9). Garnets from the three samples predominantly scatter in fields A and B of the diagram but, nonetheless, show distinct characteristics. Garnet type distribution for the three studied formations is displayed as pie charts in Figure 9.

The most diverse garnet population is present in the Tianmashan Formation with dominant input of type A (granulite-facies metasediments-70%), Bi (intermediate to felsic igneous rocks-28%), and small amounts of type Bii (amphibolite-facies metasediments -2%) garnet (Figure 9A). In contrast, the Jiaguan Formation exhibits considerably higher amounts of Bi (39%) and Bii (23%), but a lower percentage of A type (36%), grains with negligible amounts of garnet from high-grade metamafic igneous rocks (Ci type) (2%) (Figure 9B). Compositional data of garnets from sample LC-1G of the Guankou Formation suggest mainly amphibolite-facies metasediments (45%) and granulite-facies metasediments (45%) as host lithologies with only

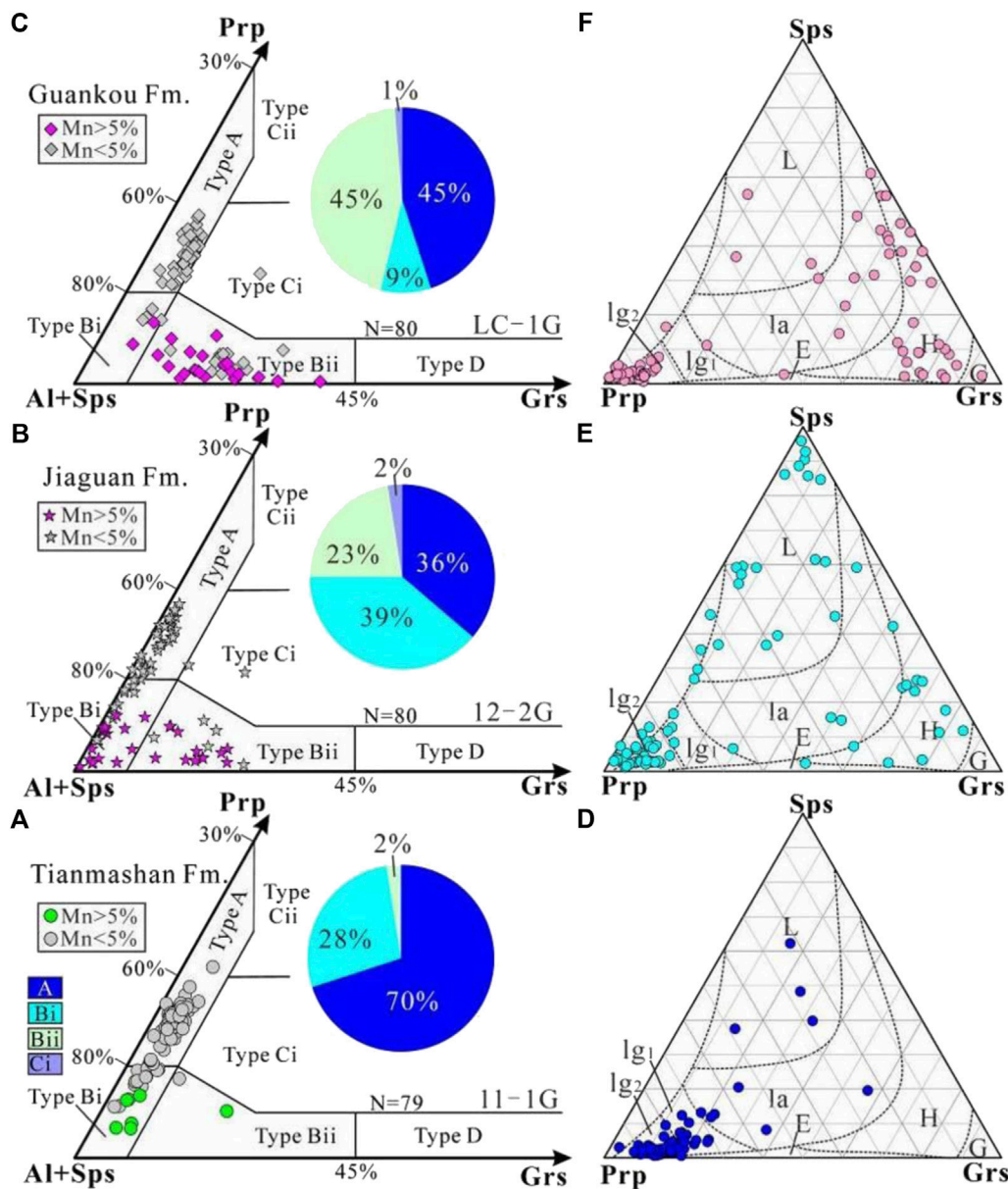


FIGURE 9

(A–C) Results of garnet chemical analysis in the ternary classification scheme of [Mange and Morton \(2007\)](#) with idealised almandine + spessartine (Alm + Sps), pyrope (Prp) and grossular (Grs) compositions as poles. Prp = pyrope, Alm = almandine, Sps = spessartine, Grs = grossular. A-sourced from granulite facies metasediments, charnockites, or intermediate to acidic deeper crust rocks; Bi-from intermediate to acidic igneous rocks; Bii-from amphibolite-facies metasediments; Ci—from high-grade metamorphic rocks; Cii—from ultramafic rocks with high Mg; D—from Ca-rich metamorphites like metasomatic rocks (skarns), very low-grade metabasic rocks or ultra-high temperature calc-silicate granulites. (D–F) Ternary discrimination diagram with proportions of pyrope, grossular, and spessartine as poles after [Teraoka et al. \(1997, 1998\)](#). L-low P–T, la -intermediate P–T (up to amphibolites facies), H—high P–T, lg1, lg2—intermediate P–T (granulite facies), E-eclogite, G-grandite garnets.

minor input of Bi (9%) and Ci (1%) type garnets (Figure 9C). Up section, type Bii garnet increased significantly.

Using the scheme of [Teraoka et al. \(1997, 1998\)](#) we see a wide range in compositions but with some coherent differences between the different samples (Figures 9D–F). The sample 11-1G has a strong preference for garnets plotting in the lg1 + lg2 (intermediate P–T, 87%) field. In contrast, sample 12-2G has some grains of that composition but some grains are biased towards common L (low P–T, 28%) and H (high P–T, 15%) garnets. More obviously, more garnet grains appeared in the la (intermediate P–T, 14%) and H (high P–T, 31%) regions of the

sample LC-1G. Almost all the samples have a significant number of grains plotting within the lg2 (intermediate-granulite facies) field. Grains plotting in the H (high P–T) field are quite common in the Guankou Formation. Such grains are rare in the Tianmashan Formation.

4.5 Detrital zircon U-Pb age

Three sandstone samples yield a total of 235 U–Pb ages with concordance within 90%–110% (Figure 10). More than 90% of the

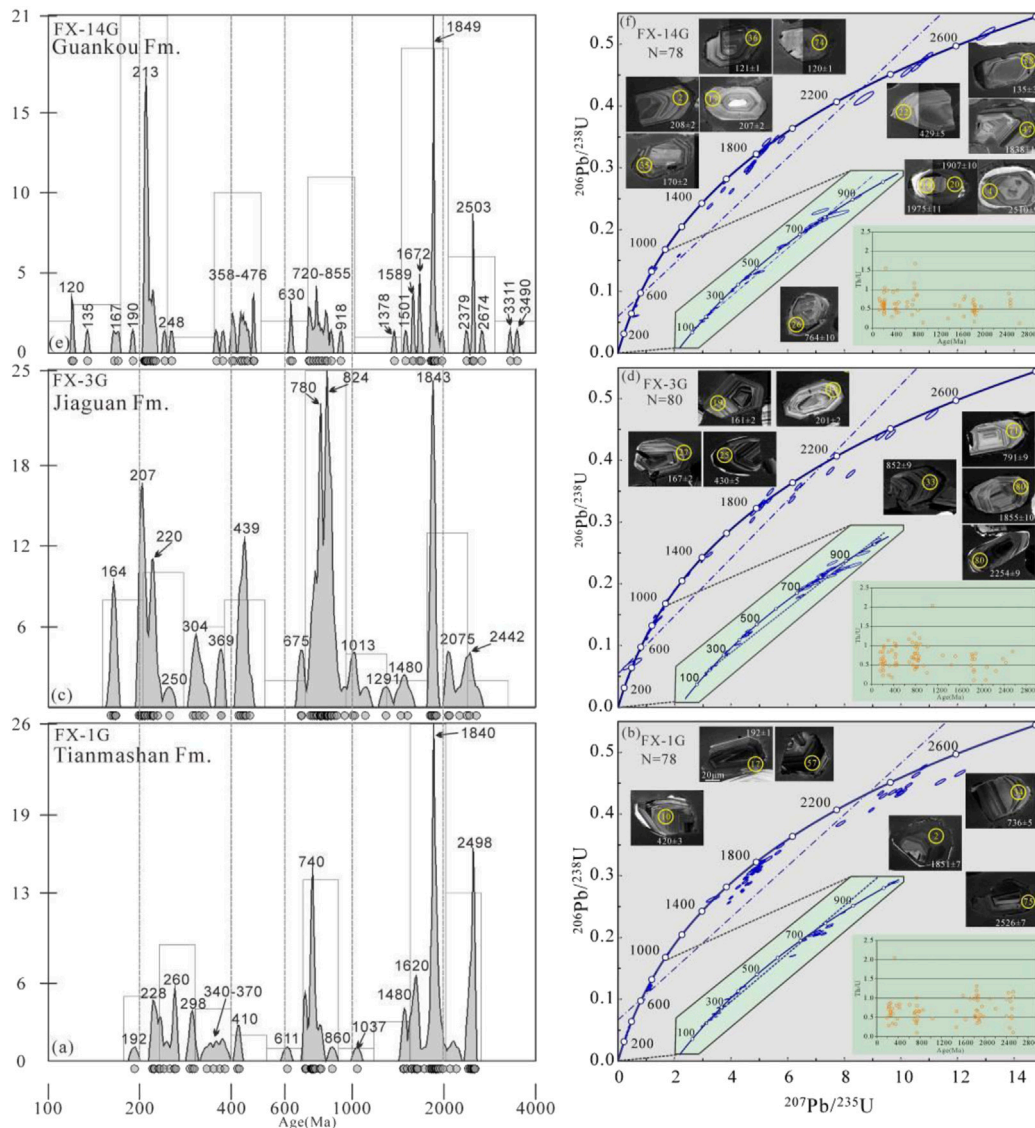


FIGURE 10

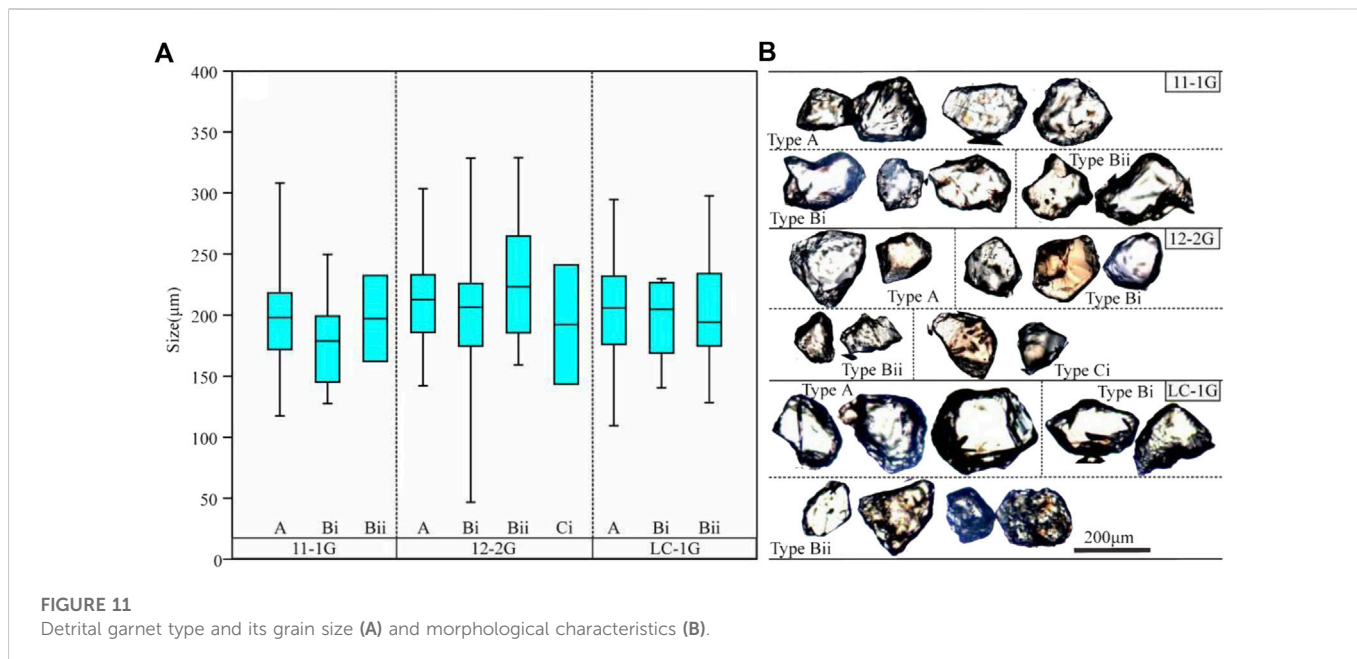
Cathodoluminescence images of the selected zircon grains and zircon U-Pb concordia and kernel density estimation (KDE) of samples of the Tianmashan Formation (A, B), Jiaguan Formation (C, D), and Guankou Formation (E, F).

zircons are short prisms, with small cores, well-developed crystal faces, and well-preserved magmatic oscillatory zoning visible in the CL images. These grains are identified as magmatic in origin and are supported by a high Th/U (> 0.2). U-Pb results (Figure 10) from three stratigraphic units are preliminarily presented in the light of stratigraphic order.

Sample FX-1G from the Early Cretaceous Tianmashan Formation. Seventy-eight grains yield six age populations of 192 Ma–240 Ma ($n=7$, 8.9%), 252 Ma–425 Ma ($n=13$, 16.7%), 700 Ma–860 Ma ($n=14$, 17.9%), 1,473 Ma–1,644 Ma ($n=9$, 11.5%), 1,731 Ma–2,098 Ma ($n=21$, 26.9%), and 2,405 Ma–2,528 Ma ($n=11$, 14.1%). The main peaks are at 740 Ma, 1840 Ma, and 2,498 Ma (Figure 10A), with three weaker peaks at age 1,620, 260, and 228 Ma. Only two zircons (grains FX-1G-68 and FX-1G-75) of 742 Ma and 2,526 Ma have low Th/U values of < 0.2 and blastoposammitic textures in the CL images, suggesting

metamorphic origin. All other grains have relatively high Th/U values and well-developed crystal faces and are identified as magmatic sources. 22% of the zircon grains have a good roundness, 26% of the zircon grains are sub-angular, and 52% of the zircon grains are angular (Figures 8, 10B).

Sample FX-3G from the Mid-Cretaceous Jiaguan Formation. Eighty zircon grains with five major age populations at 201 Ma–250 Ma ($n=13$, 16.25%), 300 Ma–461 Ma ($n=14$, 17.5%), 679 Ma–945 Ma ($n=27$, 33.75%), 1,804 Ma–1,900 Ma ($n=8$, 10%) and 161 Ma–192 Ma ($n=5$, 6.25%). Six zircon grains with ages ranging 1,006 Ma–1,521 Ma ($n=6$, 7.5%). Relative major peaks are at 164 Ma, 215 Ma, 440 Ma, 780 Ma, and 1,860 Ma (Figure 10C). Five zircon grains (6%) have round shape, blastoposammitic textures in the CL images, and relatively low Th/U values (0.11–0.18), and they are likely metamorphism origin. The remaining grains are clearly of magmatic origin, with high Th/U values of > 0.2 and well-



preserved oscillatory zoning. 9% of the zircon grains have a good roundness, 19% of the zircon grains are sub-angular, and 72% of the zircon grains are angular (Figures 8, 10D).

Sample FX-14G from the Late Cretaceous Guankou Formation. Seventy-seven grains with five major age populations at 207 Ma–242 Ma ($n = 20$, 25.97%), 1,800 Ma–1900 Ma ($n = 12$, 15.6%), 720 Ma–860 Ma ($n = 9$, 11%), 400 Ma–476 Ma ($n = 8$, 10%) and 2,509 Ma–2,674 Ma ($n = 5$, 6.49%), and three subordinate age populations of 165 Ma–190 Ma ($n = 3$, 3.89%), 120 Ma–135 Ma ($n = 3$, 3.89%), and 627–690 Ma ($n = 3$, 3.89%) (Figure 10E). Seven zircon grains with ages ranging 1,360 Ma–1,700 Ma. The sample had two dominant peak ages at 213 Ma, and 1849 Ma. Only two zircon grains (3%) have round shape, blastopsammitic textures in the CL images, and relatively low Th/U values (0.11–0.17), and they are likely metamorphism origin. The remaining grains are clearly of magmatic origin, with high Th/U values of > 0.2 and well-preserved oscillatory zoning. 5% of the zircon grains have a good roundness, 11% of the zircon grains are sub-angular, and 84% of the zircon grains are angular (Figures 8, 10F).

5 Discussion

5.1 Source analysis of garnet

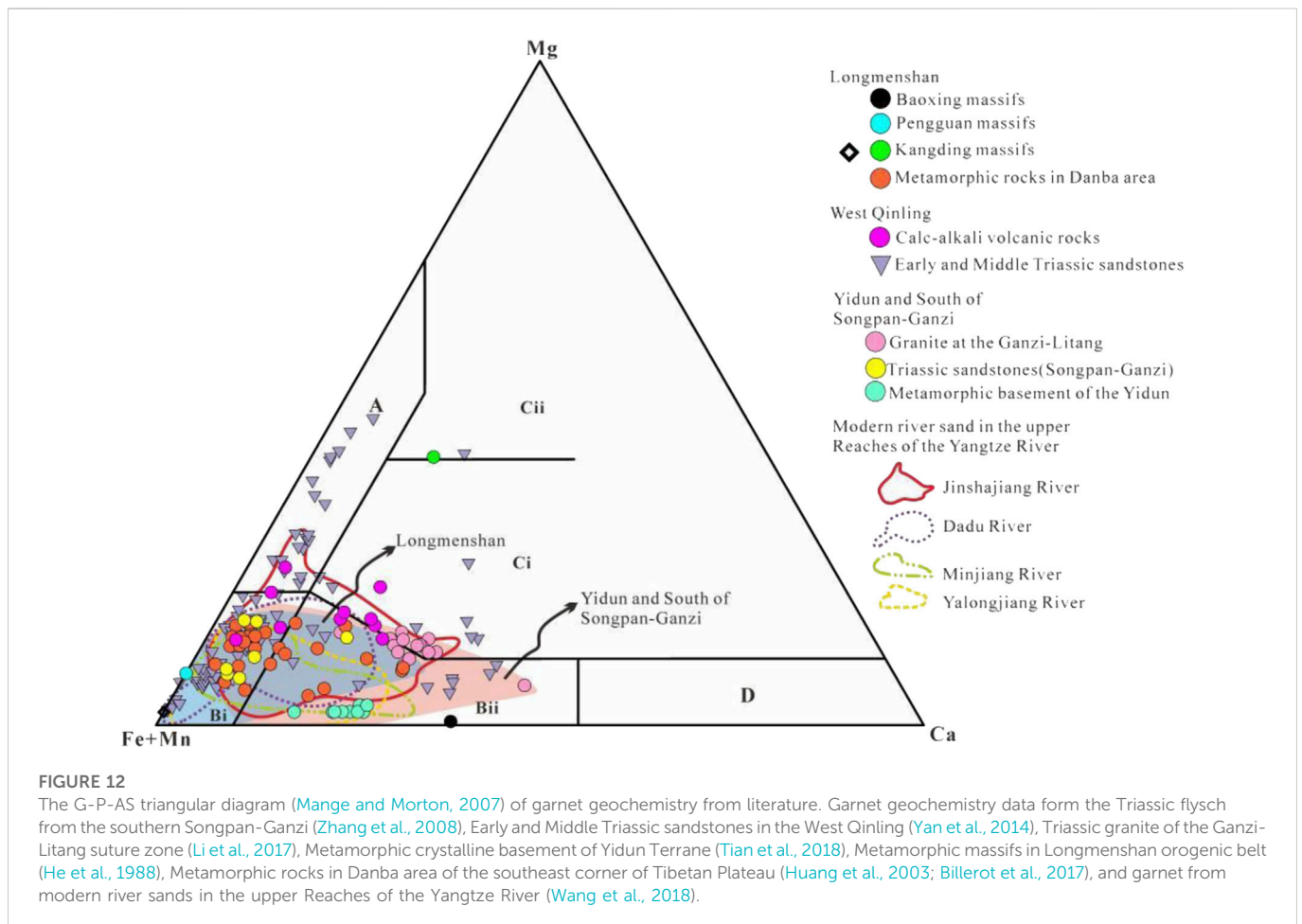
Previous studies showed that hydrodynamic has a certain effect on the separation of garnet geochemistry, thus affecting the geochemistry-based provenance interpretation (Huang et al., 2019a). Specifically, the smaller size of grains (63–125 microns) are more abundant in Fe^{2+} and Mn^{2+} , and indicate that the provenance is mainly low-level metamorphic rocks of amphibolite facies. Other larger grains (125–250 microns) have higher Ca^{2+} and Mg^{2+} , and their source rocks are more diverse including low-grade metamorphic rocks, intermediate-acid igneous rocks, and eclogite, etc. In this study, the grains size of detrital garnet is mainly distributed in the range of 110–230 microns, and most of the grains are angular and a few are

subangular-subround (Figure 11). Our analysis result shows that there was no significant difference in grain size between each type of garnet, suggesting that hydrodynamic sorting has less effect on the analysis results. It may be due to the sample itself having a similar sedimentary environment, implying the result is reliable. Therefore, the geochemical differences of garnet between samples are directly related to their provenance.

Garnets typically occur in a wide variety of metamorphic and igneous rocks, as well as in peraluminous rocks. According to the classification of Mange and Morton (2007) (Figure 9), detrital garnets from the Cretaceous sandstones are composed of type A, Bi, and Bii (Figure 9), which account for about 50%, 25.3%, and 23.4% of the analyzed garnet grains, respectively. Thus, they probably derived from granulite-facies metasedimentary rocks, intermediate to acidic igneous rocks, and amphibolite-facies metasedimentary rocks, rather than from high-grade metabasic rocks and skarns and low-grade metabasic rocks. Moreover, some low-Ca and high-Mg garnets (type A) can also be derived from charnockites and intermediate-acid igneous rocks (Sabeen et al., 2002; Morton et al., 2004). Type Bii grains are Mg- and Ca-poor but Mn-rich ($> 5\%$) garnets that most likely originated from amphibolite-facies metasedimentary rocks (Deer et al., 1997). This suggests that ultrahigh-temperature metamorphic calcisilicate granulites, amphibolite-facies metasedimentary rocks, and intermediate-acid igneous rocks are the major source of detrital garnets in the Cretaceous sandstones from the southwest corner of the Sichuan Basin.

There are three possible sources of garnet in Cretaceous sandstones in the Sichuan Basin: 1) Songpan-Ganzi Triassic flysch sediments; 2) Metamorphic basement, massifs, and amphibolite-facies metasedimentary rocks of the Longmenshan orogenic belt; 3) Recycling of older pre-Cretaceous sedimentary rocks in the Western margin of the Sichuan Basin. The possibilities and contributions of these three sources are discussed in more detail below.

Previous studies have shown that Songpan-Ganzi flysch has a multi-provenance origin, such as the east Kunlun high-grade metamorphic rock used to be one of its main source (Weislogel



et al., 2006, 2010; Enkelmann et al., 2007). The detrital garnets in Triassic flysch sediments in the West Qinling and Songpan-Ganzi fold belt are mainly type Bi (>76%) and type A (18%) (Figure 12) (Zhang et al., 2008; Yan et al., 2014). At the same time, the metamorphic strata of the Triassic in the Songpan-Ganzi metamorphic belt generally do not exceed the low green schist facies (BGMRS, 1991; Dirks et al., 1994; Brugier et al., 1997; Huang et al., 2003; Roger et al., 2010). Therefore, type Bi garnet should be the main type of garnet supplied by the Songpan-Ganzi fold belt. Our provenance analysis shows that the material supply by the Songpan-Ganzi fold belt is gradually stronger from the Lower Cretaceous Tianmashan to Upper Cretaceous Guankou Formation. Based on this, Bi type garnet should take up a higher proportion in the sediments of the Late Cretaceous, which is inconsistent with the actual analysis results.

Li et al. (2018) showed that the continental clastic rocks deposition in the Sichuan Basin had increased recirculation since the Middle Jurassic period. Although there are abundant detrital garnets in the Upper Triassic Xujiahe Formation and the Middle Jurassic Shaximiao Formation sandstones in the Sichuan Basin (An et al., 2011; Shi et al., 2011), the morphological characteristics of garnets in the Cretaceous sandstones do not support the strong recirculation deposition (Figure 11). All the heavy mineral analysis samples showed that the content of garnet in the Early Cretaceous sandstone samples was relatively low (average 3.8%), and the most obvious rich garnet sediments in the region appeared in the Upper Cretaceous Guankou Formation (this study) and Gaokanba Formation (Deng et al., 2018;

Jiang et al., 2019), whose geochemical analysis indication takes type Bii as the absolute advantage. The presence of Type A garnets in all formations is interesting. Type A garnet accounts for a major proportion (70%) in Early Cretaceous and has a similar proportion in Middle-Late Cretaceous, still maintaining at about 40% (Figure 9). They are most likely derived from high-grade granulite-facies metasedimentary rocks or charnockite and intermediate felsic igneous rock (Sabeen et al., 2002; Morton et al., 2004; Mange and Morton, 2007; Krippner et al., 2014). There was no charnockites reported from the potential source area of the Sichuan Basin.

Regional geological research shows that high-grade metamorphic complexes exist in the widely outcropping metamorphic massifs and Kangdian grey gneisses in the Longmenshan orogenic belt (SBGMR, 1982; He et al., 1988; Zhou et al., 2006b; Liu, 2006; Xu et al., 2016). Granitic gneisses, locally accompanied by variable amounts of amphibolite and garnet or amphibole two-pyroxene granulite, are the most voluminous rocks in these complexes (Zhou et al., 2006a). In the mixed gneiss of these metamorphic complexes, mainly garnet assemblage consists of pyrope, almandine, grossularite, and andradite (He et al., 1988). Moreover, the posterior mountain metamorphic belt in the Longmenshan orogenic belt is an important garnet-rich metamorphic belt in the East margin of the Tibetan Plateau (Dirks et al., 1994; Worley and Wilson, 1996; Wallis et al., 2003) (Figure 1). It is especially represented by the kyanite-sillimanite-garnet belt in Danba area and the garnet belt in the Maoxian-Wenchuan ductile shear zone (SBGMR, 1982; Worley et al., 1995). The garnet in the

Damba metamorphic complex and garnet zone is mainly almandine and a small amount of grossular (Huang et al., 2003; Billerot et al., 2017).

More importantly, the garnet geochemistry of modern river sand samples in the upper reaches of the Yangtze River reveals that the garnet produced by numerous parent rocks (magmatic rocks + metamorphic rocks) in the Yangtze River catchment is mainly type B, while type A garnet is significantly lacking (Figure 12), indicating that garnet came from the medium-low grade metamorphic rocks (Wang et al., 2018). This further confirms that the garnet supplied by the Songpan-Ganzi fold belt is mainly of type B. All of the garnets from the Triassic granite plot are close to the discrimination line between the Ci and Bii fields (Figure 12), but the garnet in the Cretaceous sandstones in the Sichuan Basin is rarely near this boundary. It is suggested that there may be few garnets from granite, while metamorphic rocks are the main provenance. The Cretaceous sandstones in the Sichuan Basin obviously lack Type C garnet, which is significantly different from the garnet type in Jurassic sandstones in the Hefei Basin, which was provided by ultrahigh pressure eclogite from the Qinling-Dabieshan orogenic belt (Li R. W. et al., 2000; Wang Q. C., 2013), indicating that the provenance areas of the Sichuan Basin are lack of high-grade basic-ultrabasic metamorphic rocks, which is also consistent with the actual geological background. In conclusion, the most likely explanation for the type A garnet is that it comes from the metamorphic complexes or relatively high-grade metamorphic rocks in the Longmenshan orogenic belt, and kyanite was detected in the Tianmashan Formation (Cao et al., 2008), which supports the interpretation of proximal high metamorphic rocks provenance. Due to its special structure-geographical location, the Longmenshan orogenic belt is not only the main provenance of the basin sediments, but also the only way for the detrital materials from western source areas to flow into the basin, so the type A garnet can be continuously reflected in the sediments. The type B garnet mainly comes from the joint contribution of the Songpan-Ganzi fold belt and the metamorphic belt of the Longmenshan orogenic belt (Figure 12). The garnet in the Late Cretaceous sediments is mainly composed of intermediate P-T metamorphic rocks, which is more suitable for the Longmenshan orogenic belt.

5.2 Interpretation of detrital zircon ages

U-Pb detrital-zircon age signatures of the Cretaceous strata of the southwest corner of the Sichuan Basin (SWCSB) contain distinct age distributions that can be linked to particular source regions (Figure 13). To assess the provenance of the Cretaceous strata preserved in the SWCSB, we include previously reported DZ results from the Jiaguan and Guankou Formation sandstones (Li et al., 2018) (Figure 2). The results obtained from the U-Pb geochronology provide a wide range of ages. Age populations occur at ~2,569 Ma–2,200 Ma, ~1,976 Ma–1,464 Ma, ~865 Ma–610 Ma, ~485 Ma–322 Ma, ~242 Ma–200 Ma, and ~167 Ma–120 Ma (Figures 10, 13). By comparing the age populations of zircons in seven sediment samples and potential source areas, the results show that the age spectra of zircons have significant temporal and spatial differences (Figure 13).

In terms of time, the Early Cretaceous Tianmashan Formation shows 2,498 Ma, 1,840 Ma, 740 Ma, and 230 Ma peaks, but the 440 Ma population is significantly lower. In the Mid-Cretaceous Jiaguan

Formation, the peak of the oldest age component (2,569 Ma–2,200 Ma) decreased or even disappeared, but the 440 Ma peak became one of the dominant age peaks. The most striking feature in the Late Cretaceous Guankou Formation is the abundance of late Triassic zircons (with a peak at 213 Ma) (Zhang et al., 2015) that are missing in Lower Cretaceous Tianmashan Formation sandstone. Spatially, the samples (G124 and 130) at the west edge of the basin were enriched to 1,840 Ma (48%–56%) at the peak, while those at 740 Ma, 440 Ma, and 230 Ma peak ages were poorer than samples at the interior of the basin (Figure 13A).

Figure 13C shows zircon age normalized probability density for the eastern margin of Tibetan Plateau units that contain ca. 2,480, 1,840 Ma, 750 Ma, 441 Ma, 260 Ma, and 230 Ma zircons, such as the Upper Triassic-Jurassic sediments in the southwestern and western Sichuan Basin (Deng et al., 2008; Chen et al., 2011; Zhang et al., 2015; Shao et al., 2016; Li et al., 2018), Triassic flysch sediments in Songpan-Ganzi fold belt (Weislogel et al., 2006, 2010; Enkelmann et al., 2007; Tang et al., 2017; Jian et al., 2019), Yidun group in the Yiduan terrane (Wang B. Q. et al., 2013), and the Longmenshan orogenic belt and Kangdian rift (Li X. H. et al., 2002; Li Z. X. et al., 2002; Li Z. X. et al., 2003; Zhou et al., 2006b; Zhao and Zhou, 2007; Zhao J. H. et al., 2008; Zhao X. F. et al., 2008; Huang et al., 2009; Sun et al., 2009; Duan et al., 2011; Wang L. J. et al., 2012; Chen et al., 2016, 2018), including the Emeishan large igneous province (Shellnutt, 2014 and references therein). It can be observed that the Yidun group has a significant peak at 970 Ma, while the early Paleozoic of Longmen shan orogenic belt includes more ages of 944 Ma and 513 Ma (Figure 13C). These ages are not obviously reflected in Cretaceous sediments in the Sichuan Basin. Meanwhile, MDS analysis shows that the above two potential sources are far away from the Cretaceous sandstone samples, indicating that they are less likely to provide clastic materials to the sediments in the Sichuan Basin (Figure 13D).

The oldest age population within the sample FX-1G from the Lower Cretaceous Tianmashan Formation illustrates Palaeoproterozoic ages, and shows bimodal characteristics (with a peak at 1,840 Ma and 2,498 Ma) (Figure 13C). The two age populations make up 52% of 78 concordant zircon ages. Although the sandstones were from the Jurassic and Upper Triassic Xujiache Formations in the western margin of the Sichuan Basin, and the Songpan-Ganzi Triassic flysch may provide zircons of 1,850 Ma and 2,500 Ma ages for the Tianmashan Formation, but the detrital materials from Songpan-Ganzi are obviously enriched with zircons of 440 Ma ages. Significant Paleoproterozoic, Neoproterozoic, and Triassic populations show similarities to Upper Triassic-Jurassic sandstones in the southwestern and western Sichuan Basin (Figure 13C), indicating that their provenance is mainly from recycling sediments, while in Early Cretaceous period Songpan-Ganzi fold belt was not the main provenance area. This also explains the high ZTR index and higher percentage of rounded zircons in the Lower Cretaceous Tianmashan Formation than in overlying strata (Figure 8).

Samples from the Jiaguan and Guankou Formations, the detrital U-Pb zircon age spectra display four major age peaks at ca. 1,840 Ma, 780 Ma–830 Ma, 440 Ma, and ca. 207 Ma–230 Ma, with two minor U-Pb age peaks at ca. 167 Ma and 2,450 Ma. The peak at ca. 240 Ma–188 Ma is consistent with the occurrence of widespread granites in the Songpan-Ganzi fold belt (Zhang et al., 2007). The major age peak encountered at ca. 860 Ma–760 Ma can be linked to the Kangdian rift. The detrital U-Pb age spectra indicate that the dominant provenance of the Jiaguan Formation sediments during

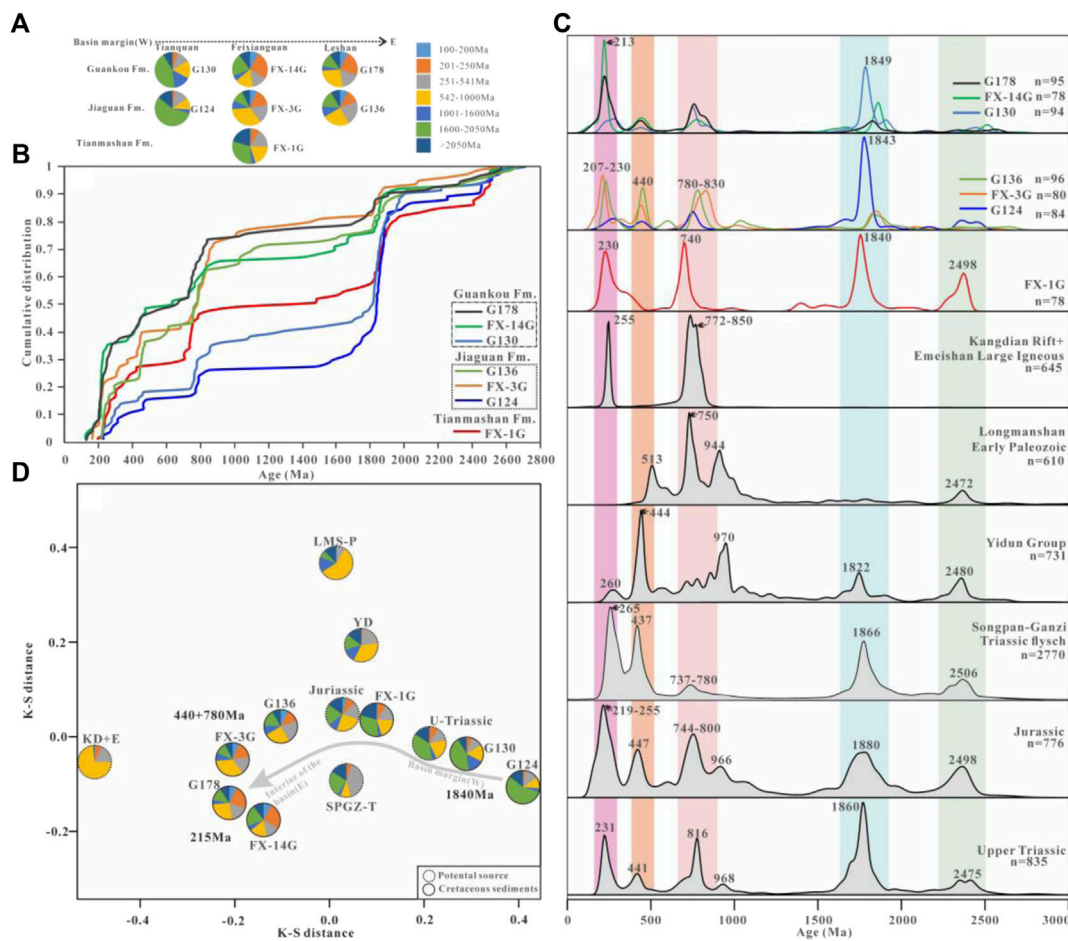


FIGURE 13

Detrital zircon U-Pb age result of the Cretaceous sediments in the Southwest corner of Sichuan Basin compared to age spectra from potential source regions. Data are shown as (A) pie diagrams, (B) cumulative distributions, (C) normalized probability density plots, and (D) a multi-dimensional scaling (MDS) plot. Data sources: Triassic flysch sediments in the Songpan-Ganzi fold belt (SPGZ-T) (Weislogel et al., 2006, 2010; Enkelmann et al., 2007; Tang et al., 2017; Jian et al., 2019); Yidun Group in the Yidun terrane (YD) (Wang B. Q. et al., 2013); Kangdian rift (late Neoproterozoic complexes: Li X. H. et al., 2002; Li Z. X. et al., 2002; Li Z. X. et al., 2003; Zhou et al., 2006a; Zhao and Zhou, 2007; Huang et al., 2009; Zhao X. F. et al., 2008; Zhao J. H. et al., 2008; Sun et al., 2009; Wang L. J. et al., 2012) and Emeishan Large Igneous Province (Shellnutt, 2014 and references therein) (KD+E); Early Paleozoic sediments from the Longmenshan orogenic belt (LMS-P): Duan et al., 2011; Chen et al., 2016, 2018; Upper Triassic sediments in southwestern and western Sichuan Basin: Deng et al. (2008), Chen et al. (2011), and Zhang et al. (2015); Jurassic sediments in the southwestern and western Sichuan Basin: Shao et al. (2016); Li et al. (2018). Cretaceous sediments (Li et al., 2018): Jiaguan Formation (G124) and Guankou Formation (G130) from Tianquan; Jiaguan Formation (G136) and Guankou Formation (G178) Formation from Leshan. The sample position is shown in Figure 2.

the Mid-Cretaceous was the Songpan-Ganzi fold belt and Longmenshan orogenic belt (Figure 13D).

5.3 Provenance change and interpretation

Using the multi-proxy provenance data, we were able to determine the provenance evolution of a thick stratigraphic succession within the southwest corner of the Sichuan Basin and two significant provenance shifts (Figure 14). The two shifts are characterized by different compositions attributed to changes in denudation areas.

Our analysis indicates that the first significant provenance change occurs at the bottom of the Mid-Cretaceous Jiaguan Formation (ca. 125 Ma) (Figure 14). This initial transition is interpreted to reflect the introduction of sediment from the Longmenshan orogenic belt and decreasing sediment input from the Pre-Cretaceous clastic rocks in the Western margin of the Sichuan Basin. Sandstones modal analysis

indicates that the lithology of the Early Cretaceous Tianmashan Formation sandstone is mainly lithic-quartz sandstone with high quartz and low plagioclase. This composition strongly indicates recycled orogen in a collision orogen as the sediment source for Tianmashan sandstones (Figure 6) (Dickinson, 1985). However, in the Jiaguan Formation sandstone, the content of microcline, plagioclase, and mica increased significantly, while the content of quartz decreased, and granite lithic fragments appeared, and few samples of Jiaguan Formation are shown in the mixed field in the Qm-F-Lt diagram, which clearly shows the composition difference with that of the Tianmashan Formation (Figure 6). Coincidentally, conglomerate clast compositions indicate from the Tianmashan Formation to the upper Jiaguan Formation, the amount of carbonate and sandstone clasts decreases while igneous and metamorphic rocks clasts increase (Figures 5, 14).

Our garnet geochemical data, based on provenance fields of idealized compositions, show that the Tianmashan Formation has more type A and less type Bii garnets than the younger Jiaguan Formation sediments

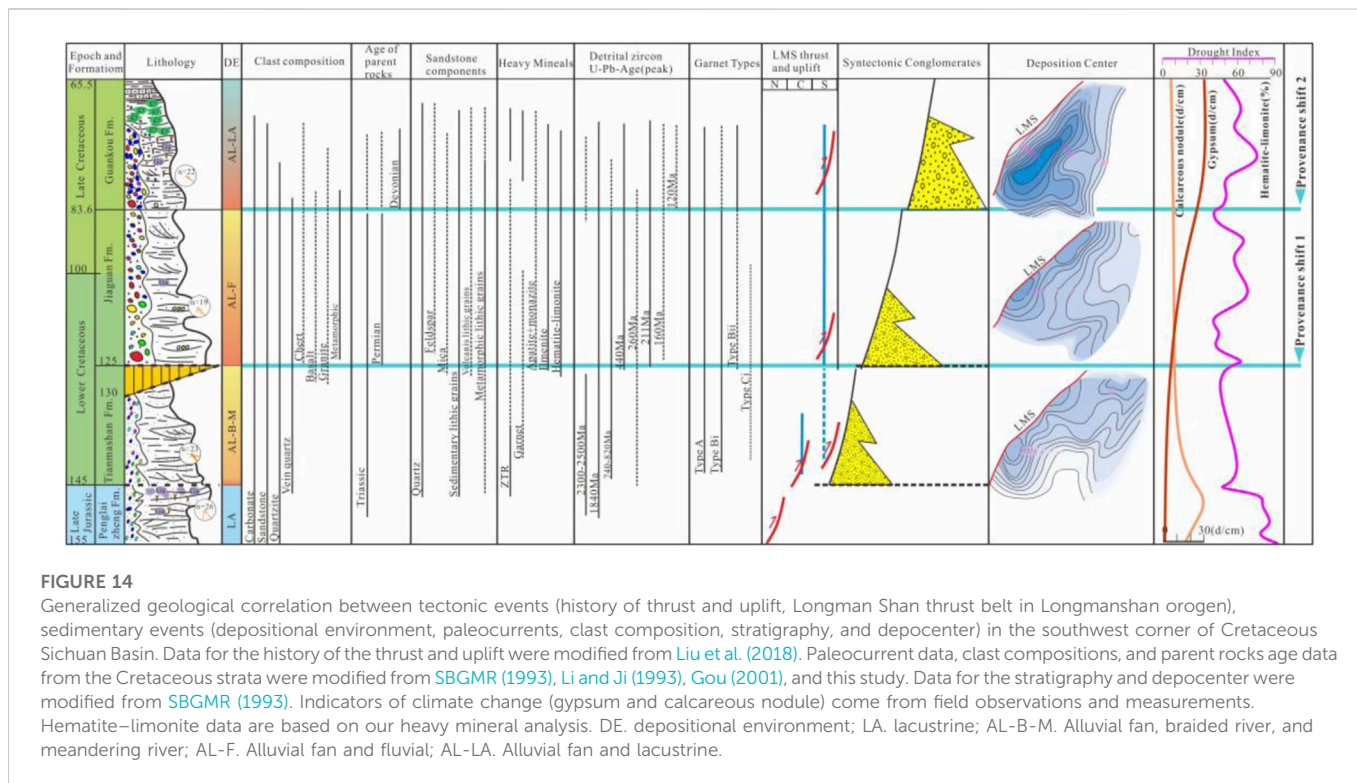


(Figure 9). This provenance shift is also indicated in the detrital zircons age distribution diagrams (Figures 10A,C). The zircon U-Pb data presented here record a dramatic change in sediment provenance from the Tianmashan Formation to the upper Jiaguan Formation, and they refine existing constraints on sediment sources for both formations, which were deposited during the transition from fluvial system to alluvial fan-braided river system in the Southwest corner of Sichuan Basin. The Tianmashan Formation zircon age population is dominated by three peaks at 740 Ma, 1,840 Ma, and 2,498 Ma (Figure 10A). By contrast, the Jiaguan Formation is dominated by ca. 164 Ma, 213 Ma, 440 Ma, ca. 800 Ma, and 1,840 Ma zircons, whereas ca. 2,440 Ma ages are minor (Figure 10B). By comparing the previous studies on Late Triassic–Late Jurassic detrital rocks in the basin and the potential provenance data (Figures 13C,D), the detrital zircon ages of the Tianmashan Formation are very consistent with the late Triassic Xujiahe Formation in the western margin of the Sichuan Basin, reflecting the bimodal characteristics of 1,840 Ma and 2,500 Ma. This indicates the migration of the erosion center from the Late Triassic Xujiahe Formation ranges to the Longmenshan orogenic belt and Songpan-Ganzi fold belt. Heavy mineral compositions support this migration: samples of Tianmashan Formation have higher ZTR values (42.58%–52%) and leucoxene with low garnet compared to that of the Jiaguan Formation. Moreover, ilmenite, monazite, and biotite with unstable physical properties are increased in the Jiaguan Formation. In addition, chromium spinel and ilmenite, which represent the basic-ultrabasic parent rocks, began to increase.

A new significant compositional change occurred in the Guankou Formation, with a Late Cretaceous age indicated by provenance shift 2. This compositional change is characterized by the increase of fossiliferous carbonate clasts and the substantial decrease of sandstone, quartzite, and vein quartz clasts (Figure 5). The content of carbonate clasts in the conglomerate can reach up to 92% (average 82%). The microfossil assemblages in the Guankou

Formation carbonate clasts are similar to the reported microfauna from the Devonian Carbonates (Gou, 2001). The unstable carbonate clasts had a shorter transport distance and were probably derived from proximal sources such as the southern section of the Longmenshan orogenic belt. This provenance change is also evidenced by the slight decrease lithic fragments of metamorphic rocks. The heavy mineral is reflected in the increase of garnet content, and the geochemical characteristics show that garnet is mainly of Type Bii, indicating that the main source is low-grade metasediments (up to amphibolite metamorphic facies). The Guankou Formation zircon age population is dominated by two peaks at 213 Ma and 1,840 Ma, with only minor Mid-Cretaceous (120 Ma–135 Ma) and Paleozoic ages (358 Ma–476 Ma), but lacking ages of 720 Ma–860 Ma. The provenance change is also reflected in the Liujia area of Yibin in southeastern Sichuan, which shows that the garnet content in the Late Cretaceous Sanhe and Gaokangba Formation is suddenly increased compared with that in the underlying strata (Deng et al., 2018; Jiang et al., 2019).

In summary, the above analyses based on multi-proxy provenance data reveal that two marked changes of sedimentary provenances occurred in the Cretaceous: a local source region for the Lower Cretaceous clastic rocks and SPGZ and LMS source regions for the Middle-Late Cretaceous successions.

5.4 Implication for mid-cretaceous rapid denudation of Eastern Tibetan plateau

Cretaceous strata of the southwestern corner of the Sichuan Basin provide an excellent opportunity to decipher changes in sediment provenance during the transition from Longmenshan thrusting through the formation of regional Cretaceous Plateau uplifts.

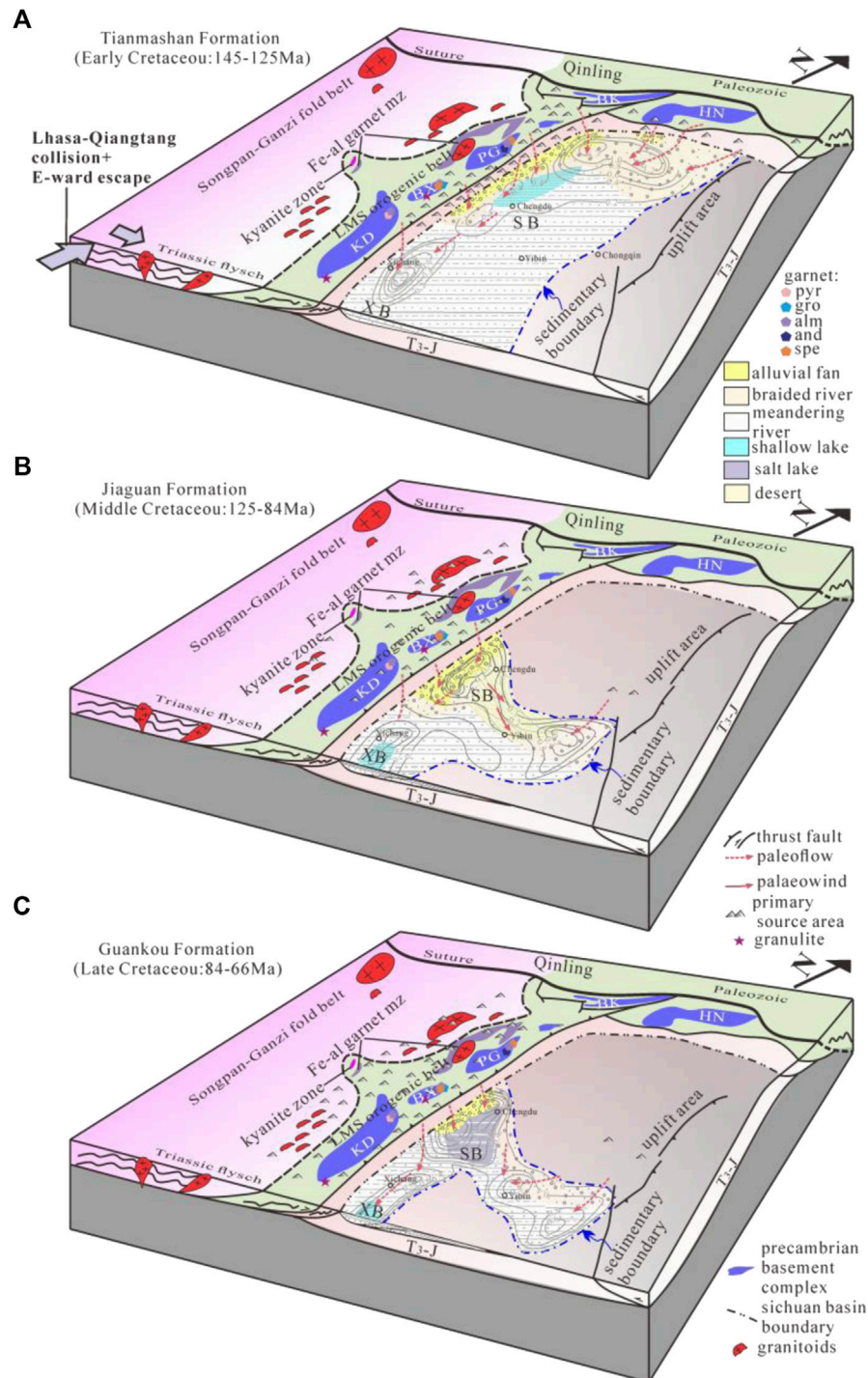


FIGURE 15

Schematic block diagrams illustrating exhumation history of the East margin of Tibetan Plateau, and tectono-sedimentary evolution of its foreland basin.

(A) Early Cretaceous, (B) Middle Cretaceous, and (C) Late Cretaceous. Isopach maps after Guo et al. (1996). HN, Hannan; BK, Bikou; KD, Kangdian; BX, Baoxing. PG, Pengguan; mz, metamorphic zone; SB, Sichuan Basin; XB, Xichang Basin.

Our detailed provenance analysis revealed that two provenance shifts were located at the bottom of the Jianguan Formation and within the Guankou Formation, respectively (Figure 14). The two provenance changes were accompanied by the change of sedimentary environment from fluvial facies to alluvial fan and alluvial fan-lacustrine sedimentary systems (Gou, 1998; Gou, 2001).

Abrupt shifts in sediment provenance at geologic timescales can be an indication of tectonic reconfiguration of upland source areas (Horton et al., 2004). A Cretaceous palaeogeographic reconstruction with major sediment transport directions (Figure 15) shows suggested sources for Cretaceous in the Sichuan Basin that are SPGZ, LMS, and pre-Cretaceous sediments in the west edge of the Sichuan Basin. The changes in sedimentary facies and provenance indicate that the eastern

margin of the Tibetan Plateau has become the main provenance area of Cretaceous clastic rocks, and rapid uplift and denudation began to occur during the sedimentary period of the Jiaguan Formation. In other words, intense tectonic activity began in the eastern margin of the Tibetan Plateau began from Middle Cretaceous (125 Ma).

Tectonic reconstructions indicate that the Mountain Frontal Fault (Beichaun Fault), involving crystalline basement at depth, would have been most reactive during the Lower Cretaceous Tianmashan and Jiaguan syntectonic depositions, as observed at Pengguan massif (Airaghi et al., 2017b). There is a good agreement between the uplift denudation events of sedimentary records and cooling events of the Cretaceous at the eastern margin of the Tibetan Plateau revealed by low-temperature thermochronology (Liu et al., 2018).

Reviewing the history of regional tectonic evolution, the most important tectonic transformation occurred in the late Early Cretaceous, when the tectonic environment of the Sichuan Basin changed from the Qinling tectonic domain to the Tibetan Plateau tectonic domain (Liu et al., 2013a; Liu et al., 2018). On the one hand, the tectonic nature of the Qinling orogenic belt has undergone a major transformation and the structural deformation of the northwestern boundary of the basin and the northern part of the basin was basically finalized in this event, and the deposition has since ended and entered a state of uplift and denudation. Since then, the tectonic activities of the Qinling orogenic belt have no significant influence on the western Sichuan foreland basin. At the same time, affected by the long-range effects of the collision between the Lhasa and Qiangtang terranes and the collision between the Indian plate and the Eurasian plate, the central and southern section of Longmen mountains, became active again, forming a new foredeep on its front edge. The subsidence center migrated from early northwestern Sichuan to southwestern Sichuan, and then entered the Late Cretaceous to Paleogene foreland basin evolution stage under the control of the Tibetan Plateau tectonic domain. The regional uplift in the late Early Cretaceous made the Lower Cretaceous in the northern part of the basin and the Tianmashan Formation in the southern part of the basin suffered different degrees of denudation. During the deposition of the Jiaguan Formation, the depositional range was reduced, and the basin turned into a differential evolution stage of north uplift-south down. The provenance transition of the Guankou Formation responded to the late Cretaceous period (~80 Ma) with another significant uplift and denudation of Longmen Mountain at the eastern edge of the Tibetan Plateau.

6 Conclusion

Based on sedimentology and new provenance data from the Early Cretaceous Tianmashan Formation to Late Cretaceous Guankou Formation together with a thorough literature compilation, we conclude as follows:

- 1) Detrital garnet geochemistry of three Cretaceous sandstone samples from Feixianguan outcrop show distinct characteristics. The detrital garnets from the Tianmashan Formation with dominant input of type A and Bi, while the Jiaguan and Guankou Formations have significantly increased Bii type. Our results indicated the intermediate P-T metamorphic rocks had uplifted and suffered from erosion in the eastern Tibetan Plateau during the Mid-Cretaceous.
- 2) Major provenance changes were observed at 125 Ma and 80 Ma. Denudation of the SPGZ occurred after 125 Ma resulting in the change in the sediment source from the Triassic in the

Longmenshan orogenic belt front to flysh sediments of the SPGZ. After 80 Ma, considerable amounts of sediments were supplied from the Longmenshan orogenic belt.

- 3) The significant surface uplift and rapid denudation of the eastern margin of the Tibetan Plateau were probably initiated in the mid-Cretaceous (~120 Ma).

Data availability statement

The datasets presented in this study can be found in online repositories. The names of the repository/repositories and accession number(s) can be found in the article/Supplementary Material.

Author contributions

ZW and SL conceived and designed the study. ZJ measured Chronological data and wrote the first draft of the manuscript. BR and JX provided constructive suggestions to improve the work. WH, YH, KT, and TH edited and reviewed the manuscript.

Funding

This study was financially supported by the National Natural Science Foundation of China (No. 42230310).

Acknowledgments

We thank Bin Deng and Chihua Wu from Chengdu University of Technology for constructive advice, as well as Lei Jiang for his field assistance. And we thank the reviewers for the review suggestions for this work.

Conflict of interest

The authors declare that the research was conducted in the absence of any commercial or financial relationships that could be construed as a potential conflict of interest.

Publisher's note

All claims expressed in this article are solely those of the authors and do not necessarily represent those of their affiliated organizations, or those of the publisher, the editors and the reviewers. Any product that may be evaluated in this article, or claim that may be made by its manufacturer, is not guaranteed or endorsed by the publisher.

Supplementary material

The Supplementary Material for this article can be found online at: <https://www.frontiersin.org/articles/10.3389/feart.2023.1113377/full#supplementary-material>

References

- Airaghi, L. (2017a). "A petro-chronological study of the longmen Shan thrust belt (eastern tibet): Geological inheritance and implication for the present geodynamics," in *Earth sciences* (Université Grenoble Alpes). English. <NNT: 2017GREAU029>. <tel-01712320>.
- Airaghi, L., De Sigoyer, J., Lanari, P., Guillot, S., Vidal, O., Monie, P., et al. (2017b). Total exhumation across the Beichuan fault in the longmen Shan (eastern Tibetan plateau, China): Constraints from petrology and thermobarometry. *J. Asian Earth sciences* 140, 108–121.
- Airaghi, L., Sigoyer, J., Guillot, S., Robert, A., Warren, C. J., and Deldicque, D. (2018). The Mesozoic along-strike tectono-metamorphic segmentation of Longmen Shan (eastern Tibetan plateau). *Tectonics* 37, 4655–4678. doi:10.1029/2018tc005005
- Allen, P. A. (2017). *Sediment routing systems: The fate of sediment from source to sink*. Cambridge, UK: Cambridge University Press.
- An, H. Y., Shi, Z. Q., Zhang, H. J., Zeng, D. Y., and Zhong, H. (2011). On material source of sandstone reservoir of the middle jurassic Shaximiao Formation in west sichuan depression. *J. Sichuan Geol.* 31 (1), 29–33. (in Chinese with English abstract).
- Andersen, T. (2002). Correction of common lead in U–Pb analyses that do not report 204Pb. *Chem. Geol.* 192, 59–79. doi:10.1016/s0009-2541(02)00195-x
- Arne, D., Worley, B., Wilson, C., Chen, S. F., Foster, D., Luo, Z. L., et al. (1997). Differential exhumation in response to episodic thrusting along the eastern margin of the Tibetan Plateau. *Tectonophysics* 280, 239–256. doi:10.1016/s0040-1951(97)00040-1
- Baral, U., Lin, D., and Chamlagain, D. (2017). Detrital zircon ages and provenance of Neogene foreland basin sediments of the Karnali River section, Western Nepal Himalaya. *J. Asian Earth Sci.* 138, 98–109. doi:10.1016/j.jseas.2017.02.003
- Billerot, A., Duchene, S., Vanderhaeghe, O., and de Sigoyer, J. (2017). Gneiss domes of the Danba metamorphic complex, songpan ganze, eastern tibet. *J. Asian Earth Sci.* 140, 48–74. doi:10.1016/j.jseas.2017.03.006
- Brugier, O., Lancelot, J. R., and Malavieille, J. (1997). U–Pb dating on single detrital zircon grains from the triassic songpan–ganze flysch (central China): Provenance and tectonic correlations. *Earth Planet. Sci. Lett.* 152 (1–4), 217–231. doi:10.1016/s0012-821x(97)00138-6
- Burchfiel, B. C., Chen, Z., Liu, Y., and Royden, L. H. (1995). Tectonics of the Longmen Shan and adjacent regions, central China. *Int. Geol. Rev.* 37, 661–735. doi:10.1080/00206819509465424
- Bureau of Geology and Mineral Resources of Sichuan Province (BGMRS) (1991). *Regional geology of sichuan province*. Beijing: Geological Publishing House, 1–730. (in Chinese).
- Cao, K., Li, X. H., and Wang, C. S. (2008). The cretaceous clay minerals and paleoclimate in Sichuan Basin. *Acta Geol. Sin.* 82 (1), 115–123.
- Cawood, P. A., Hawkesworth, C. J., and Dhuime, B. (2012). Detrital zircon record and tectonic setting. *Geology* 40 (10), 875–878. doi:10.1130/g32945.1
- Cawood, P. A., and Nemchin, A. A. (2000). Provenance record of a rift basin: U/Pb ages of detrital zircons from the perth basin, western Australia. *Sediment. Geol.* 134 (3–4), 209–234. doi:10.1016/s0037-0738(00)00044-0
- Chang, E. Z. (2000). Geology and tectonics of the Songpan–Ganzi fold belt, southwestern China. *Int. Geol. Rev.* 42 (9), 813–831. doi:10.1080/00206810009465113
- Chen, H. L., Zhu, M., Chen, S. Q., Xiao, A. C., Jia, D., and Yang, G. (2020). Basin-orogen patterns and the late Triassic foreland basin conversion process in the Western Yangtze Block, China. *J. Asian Earth Sci.* 194, 104311. doi:10.1016/j.jseas.2020.104311
- Chen, P. J. (1983). A Survey of the non-marine cretaceous in China. *Cretaceous Research* 4, 123–143.
- Chen, Q., Sun, M., Long, X. P., Zhao, G. C., Wang, J., Yu, Y., et al. (2018). Provenance study for the paleozoic sedimentary rocks from the West yangtze block: Constraint on possible link of Southsouth China to the gondwana supercontinent reconstruction. *Precambrian Res.* 309, 271–289. doi:10.1016/j.precamres.2017.01.022
- Chen, Q., Sun, M., Long, X., Zhao, G., and Yuan, C. (2016). U–Pb ages and Hf isotopic record of zircons from the late neoproterozoic and silurian–devonian sedimentary rocks of the Western yangtze block: Implications for its tectonic evolution and continental affinity. *Gondwana Res.* 31, 184–199. doi:10.1016/j.gr.2015.01.009
- Chen, S. F., Wilson, C. J. L., and Worley, B. A. (1995). Tectonic transition from the Songpan–Garzê fold belt to the Sichuan Basin, south-Western China. *Basin Res.* 7, 235–253. doi:10.1111/j.1365-2117.1995.tb00108.x
- Chen, Y., Liu, S. G., Li, Z. W., Deng, B., Zeng, X. L., and Lin, J. (2011). LA-ICP-MS detrital zircon u–pb geochronology approaches to the sediment provenance of the Western Sichuan Foreland Basin and limited uplift of the Longmen Mountains during the Early stage of Late Triassic. *Geotect. Metallogenia* 35 (2), 315–323.
- Chengdu Institute of Geology and Mineral Resources (CGMR) (1979). *Stratigraphic summary of southwest China (cretaceous)*, 1–176.
- Chung, S. L., Lo, C. H., Lee, T. Y., Zhang, Y. Q., Xie, Y. W., Li, X. H., et al. (1998). Diachronous uplift of the Tibetan plateau starting 40 Myr ago. *Nature* 394, 769–773. doi:10.1038/29511
- Compiling Group of Continental Mesozoic Stratigraphy and Palaeontology in Sichuan Basin of China (1982). *Continental mesozoic stratigraphy and paleontology in sichuan Basin of China*. Chengdu: People's Publishing House of Sichuan, 5–235.
- DeCelles, P. G., and Giles, K. A. (1996). Foreland basin systems. *Basin Res.* 8, 105–123. doi:10.1046/j.1365-2117.1996.01491.x
- DeCelles, P. G., Langford, R. P., and Schwartz, R. K. (1983). Two new methods of paleocurrent determination from trough cross-stratification. *J. Sediment. Petrology* 53, 629–642.
- Deer, W. A., Howie, R. A., and Zussman, J. (1992). *Rock-forming minerals*. Harlow, UK: Longman Group Ltd., 712.
- Deer, W. A., Howie, R. A., and Zussman, J. (1997). *Rock-forming minerals volume 2B Double-chain silicates*. 2nd ed. London: The Geol. Soc., 784.
- Deng, B., David, C., Jiang, L., Mark, C., Cogné, N., Wang, Z. J., et al. (2018). Heavy mineral analysis and detrital u–pb ages of the intracontinental paleo-yanagzte basin: Implications for a transcontinental source-to-sink system during late cretaceous time. *Geol. Soc. Am. Bull.* 130 (11–12), 2087–2109. doi:10.1130/b32037.1
- Deng, B., Liu, S. G., Jansa, L., Yong, S., and Zhang, Z. (2013a). Fractal analysis of veins in permian carbonate rocks in the lingtanchang anticline, western China. *Geofluids* 14 (2), 160–173. doi:10.1111/gfl.12059
- Deng, B., Liu, S. G., Li, Z. W., Jansa, L., Liu, S., Wang, G. Z., et al. (2013b). Differential exhumation at eastern margin of the Tibetan plateau, from apatite fission-track thermochronology. *Tectonophysics* 591, 98–115. doi:10.1016/j.tecto.2012.11.012
- Deng, F., Jia, D., Luo, L., Li, H. B., Li, Y. Q., and Wu, L. (2008). The contrast between provenances of songpan–ganze and Western sichuan foreland basin in the late triassic: Clues to the tectonics and paleogeography. *Geol. Rev.* 54, 561–573. (in Chinese with English abstract). doi:10.16509/j.georeview.2008.04.005
- Dickinson, W. R., Beard, L. S., Brakenridge, G. R., Erjavić, J. L., Ferguson, R. C., Inman, K. F., et al. (1983). Provenance of North American Phanerozoic sandstones in relation to tectonic setting. *Geol. Soc. Am. Bull.* 94, 222–235. doi:10.1130/0016-7606(1983)94<222:ponaps>2.0.co;2
- Dickinson, W. R. (1970). Interpreting detrital modes of graywacke and arkose. *J. Sediment. Petrology* 40, 695–707.
- Dickinson, W. R. (1985). "Interpreting provenance relations from detrital modes of sandstones," in *Provenance of arenites. NATO ASI series, mathematical and physical sciences*. Editor G. G. Zuffa, 148, 333–361.
- Dickinson, W. R. (1988). "Provenance and sediment dispersal in relation to paleotectonics and paleogeography of sedimentary basins," in *New perspectives in basin analysis*. Editors K. L. Kleinspehn and C. Paola (New York, NY: Springer), 3–25.
- Dickinson, W. R., and Suczek, C. A. (1979). Plate tectonics and sandstone compositions. *Am. Assoc. Petroleum Geol. Bull.* 63, 2164–2182.
- Ding, L., Kapp, P., Cai, F., Garzzone, C. N., Xiong, Z., Wang, H., et al. (2022). Timing and mechanisms of Tibetan Plateau uplift. *Nat. Rev. Earth Environ* 3, 652–667. doi:10.1038/s43017-022-00318-4
- Ding, L., Spicer, R. A., Yang, J., Xu, Q., Cai, F., Li, S., et al. (2017). Quantifying the rise of the Himalaya orogen and implications for the south Asian monsoon. *Geology* 45 (3), 215–218. doi:10.1130/g38583.1
- Ding, L., Yang, D., Cai, F. L., Pullen, A., Kapp, P., Gehrels, G. E., et al. (2013). Provenance analysis of the mesozoic hoh-xil-songpan-ganzi turbidites in northern tibet: Implications for the tectonic evolution of the eastern paleo-tethys ocean. *Tectonics* 32, 34–48. doi:10.1002/tect.20013
- Dirks, P. H. G. M., Wilson, C. G. L., Chen, S. F., Luo, Z. L., and Liu, S. G. (1994). Tectonic evolution of the NE margin of the Tibetan plateau: Evidence from the central longmenshan, sichuan province, China. *J. Southeast Asian Earth Sci.* 9, 181–192. doi:10.1016/0743-9547(94)90074-4
- Druschke, P., Hanson, A. D., Yan, Q., Wang, Z. Q., and Wang, T. (2006). Stratigraphic and U–Pb SHRIMP detrital zircon evidence for a Neoproterozoic continental arc, Central China: Rodinia implications. *J. Geol.* 114, 627–636. doi:10.1086/506162
- Duan, L., Meng, Q. R., Zhang, C. L., and Liu, X. M. (2011). Tracing the position of the southsouth China block in gondwana: U–Pb ages and Hf isotopes of devonian detrital zircons. *Gondwana Res.* 19, 141–149. doi:10.1016/j.gr.2010.05.005
- Enkelmann, E., Weislogel, A., Ratschbacher, L., Eide, E., Renno, A., and Wooden, J. (2007). How was the triassic songpan-ganze basin filled? A provenance study. *Tectonics* 26. doi:10.1029/2006TC002078
- Enkin, R. J., Courtillot, V., Xing, L., Zhang, Z., Zhuang, Z., and Zhang, J. (1991). The stationary Cretaceous paleomagnetic pole of Sichuan (south China block). *Tectonics* 10 (3), 547–559. doi:10.1029/90tc02554
- Feo-Codecido, G. (1956). Heavy-mineral techniques and their application to Venezuelan stratigraphy. *Am. Assoc. Petroleum Geol. Bull.* 40, 984–1000.
- Fielding, E. J. (1996). Tibet uplift and erosion. *Tectonophysics* 260, 55–84. doi:10.1016/0040-1951(96)00076-5
- Garzanti, E., Doglioni, C., Vezzoli, G., and Ando, S. (2007). Orogenic belts and orogenic sediment provenance. *J. Geol.* 115, 315–334. doi:10.1086/512755
- Gehrels, G. (2014). Detrital zircon U–Pb geochronology applied to tectonics. *Annu. Rev. Earth Planet. Sci.* 42, 127–149. doi:10.1146/annurev-earth-050212-124012
- Gong, D. X., Wu, C. H., Zou, H., Zhou, X., Zhou, Y., Tan, H. Q., et al. (2021). Provenance analysis of late triassic turbidites in the eastern songpan–ganzi flysch complex:

- Sedimentary record of tectonic evolution of the eastern Paleotethys ocean. *Mar. Petroleum Geol.* 126, 104927. doi:10.1016/j.marpetgeo.2021.104927
- Gou, Z. H. (2001). Characteristics of Jurassic-Tertiary conglomerates and depositional environment in the Dayi-Wenchuan area, Sichuan. *Regional Geol. China* 17 (2), 124–131. (in Chinese with English abstract).
- Gou, Z. H. (1998). The Jurassic-Cretaceous in the Yaan-Baoxing area, Sichuan. *Regional Geol. China* 20 (1), 25–32. (in Chinese with English abstract).
- Guo, Z. W., Deng, K. L., and Han, Y. F. (1996). *Formation and evolution of the Sichuan Basin*. Beijing: Geologic Publishing House.
- Harland, W. B., Cox, A. V., Llewellyn, P. G., Pickton, C. A., Smith, A. G., and Walsted, R. (1982). *A geologic time scale*. New York: Cambridge University Press.
- Harrowfield, M. J., and Wilson, C. J. L. (2005). Indosinian deformation of the Songpan Garzê fold belt, northeast Tibetan plateau. *J. Struct. Geol.* 27 (1), 101–117. doi:10.1016/j.jsg.2004.06.010
- Hartley, A. J., and Otava, J. (2001). Sediment provenance and dispersal in a deep marine foreland basin: The Lower Carboniferous Culm Basin, Czech Republic. *J. Geol. Soc. Lond.* 158, 137–150. doi:10.1144/jgs.158.1.137
- He, J. M., Chen, G. H., Yang, Z. L., Min, J. K., and Liu, Q. X. (1988). *The Kangdian gray gneisses*. Chongqing: Chengdu Institute of Geology and Mineral Resources Chongqing Publishing House. (in Chinese with English abstract).
- Hong, D. M., Jian, X., Fu, L., and Zhang, W. (2020b). Garnet trace element geochemistry as a sediment provenance indicator: An example from the Qaidam basin, northern Tibet. *Mar. Petroleum Geol.* 116, 104316. doi:10.1016/j.marpetgeo.2020.104316
- Hong, D. M., Jian, X., Huang, X., Zhang, W., and Ma, J. G. (2020a). Garnet trace elemental geochemistry and its application in sedimentary provenance analysis. *Earth Sci. Front.* 27 (3), 191–201. (in Chinese with English abstract). doi:10.13745/j.esf.2020.1.1
- Horton, B. K., Constenius, K. N., and DeCelles, P. G. (2004). Tectonic control on coarse-grained foreland-basin sequences: An example from the Cordilleran foreland basin, Utah. *Utah. Geol.* 32, 637–640. doi:10.1130/g20407.1
- Huang, H. Y., He, D. F., Li, D., and Li, Y. D. (2019a). Detrital zircon U-Pb ages of Paleogene deposits in the southwestern Sichuan foreland basin, China: Constraints on basin-mountain evolution along the southeastern margin of the Tibetan Plateau. *Geol. Soc. Am. Bull.* 131 (3–4), 668–686. doi:10.1130/b35211.1
- Huang, M. H., Buick, I. S., and Hou, L. W. (2003). Tectonometamorphic evolution of the eastern Tibet plateau: Evidence from the central Songpan-Garze orogenic belt, western China. *J. Petrology* 44 (2), 255–278. doi:10.1093/petrology/44.2.255
- Huang, T. K., and Chen, B. W. (1987). *The evolution of the tethys in China and adjacent regions*. Beijing: Geological Publishing House, 108–109. (in Chinese).
- Huang, X., Jian, X., Zhang, W., Hong, D. M., Guan, P., and Du, J. X. (2019b). Detrital garnet geochemistry-based provenance analysis and interpretation: The effect of grain size. *Acta Sedimentol. Sin.* 37 (3), 511–518. (in Chinese with English abstract). doi:10.14027/j.issn.1000.0550.2018.161
- Huang, X. L., Xu, Y. G., Lan, J. B., Yang, Q. J., and Luo, Z. Y. (2009). Neoproterozoic adakitic rocks from mopanshan in the Western Yangtze craton: Partial melts of a thickened lower crust. *Lithos* 112, 367–381. doi:10.1016/j.lithos.2009.03.028
- Hubert, J. F. (1962). A zircon-tourmaline-rutile maturity index and the interdependence of the composition of heavy mineral assemblages with the gross composition and texture of sandstones. *J. Sediment. Petrology* 32, 440–450.
- Ingersoll, R. V., Fullard, T. F., Ford, R. L., Grimm, J. P., Pickle, J. D., and Sares, S. W. (1984). The effect of grain size on detrital modes; a test of the Gazzi-Dickinson point-counting method. *J. Sediment. Res.* 54, 103–116.
- Ingersoll, R. V., and Suczek, C. A. (1979). Petrology and provenance of neogene sand from nicobar and bengal fans, dsdp sites 211 and 218. *J. Sediment. Res.* 49 (4), 1228–1271.
- Jackson, W. T., Jr., Robinson, D. M., Weislogel, A. L., Jian, X., and McKay, M. P. (2018a). Cenozoic development of the nonmarine Mula basin in the Southern Yidun terrane: Deposition and deformation in the eastern Tibetan Plateau associated with the India-Asia collision. *Tectonics* 37, 2446–2465. doi:10.1029/2018TC004994
- Jackson, W. T., Jr., Robinson, D. M., Weislogel, A. L., Shang, F., and Jian, X. (2018b). Mesozoic development of nonmarine basins in the northern Yidun terrane: Deposition and deformation in the eastern Tibetan Plateau prior to the India-Asia collision. *Tectonics* 37, 2466–2485. doi:10.1029/2018TC004995
- Ji, X. T., and Li, Y. L. (1995). Alluvial fan-lake facies association in the late Cretaceous-Paleogene continental basin of the Tianquan-Lushan area. *J. Chengdu Inst. Technol.* 22 (02), 15–21. (in Chinese with English abstract).
- Jia, D., Wei, G. Q., Chen, Z. X., Li, B. L., Zeng, Q., and Yang, G. (2006). Longmen Shan fold-thrust belt and its relation to the Western Sichuan Basin in central China: New insights from hydrocarbon exploration. *AAPG* 90, 1425–1447. doi:10.1306/03230605076
- Jian, X., Guan, P., Zhang, D. W., Zhang, W., Feng, F., Liu, R. J., et al. (2013). Provenance of Tertiary sandstone in the northern Qaidam basin, northeastern Tibetan Plateau: Integration of framework petrography, heavy mineral analysis and mineral chemistry. *Sediment. Geol.* 290, 109–125. doi:10.1016/j.sedgeo.2013.03.010
- Jian, X., Weislogel, A., and Pullen, A. (2019). Triassic sedimentary filling and closure of the eastern paleo-tethys ocean: New insights from detrital zircon geochronology of songpan-ganzi, Yidun, and West Qinling flysch in eastern Tibet. *Tectonics* 38, 767–787. doi:10.1029/2018TC005300
- Jiang, L., Liu, S. G., Wang, Z. J., Li, Z. W., Lai, D., He, Y., et al. (2019). Provenance change and its indication of late cretaceous in the west margin of upper yangtze basin. *Geol. Rev.* 65 (2), 477–490. (in Chinese with English abstract). doi:10.16509/j.georeview.2019.02.017
- Kamp, P. J., Liu, S. G., Xu, G. Q., Li, Z. W., Danisik, M., and Deng, B. (2013). Cooling history of a crustal section in eastern Tibet (well HC1) constrained by thermochronology. *Acta Geol. Sin.*, 57–58. (English Edition) 87(supp).
- Krippner, A., Meinhold, G., Morton, A. C., Russell, E., and von Eynatten, H. (2015). Grain-size dependence of garnet composition revealed by provenance signatures of modern stream sediments from the Western Hohe Tauern (Austria). *Sediment. Geol.* 321, 25–38. doi:10.1016/j.sedgeo.2015.03.002
- Krippner, A., Meinhold, G., Morton, A. C., Schönig, J., and von Eynatten, H. (2016). Heavy minerals and garnet geochemistry of stream sediments and bedrocks from the Almklodalen area, western gneiss region, SW Norway: Implications for provenance analysis. *Sediment. Geol.* 336, 96–105. doi:10.1016/j.sedgeo.2015.09.009
- Krippner, A., Meinhold, G., Morton, A. C., and von Eynatten, H. (2014). Evaluation of garnet discrimination diagrams using geochemical data of garnets derived from various host rocks. *Sediment. Geol.* 306, 36–52. doi:10.1016/j.sedgeo.2014.03.004
- Lenaza, D., Mazzolli, C., Velicogna, M., and Princivalle, F. (2018). Trace and Rare Earth Elements chemistry of detrital garnets in the SE Alps and Outer Dinarides flysch basins: An important tool to better define the source areas of sandstones. *Mar. Petroleum Geol.* 98, 653–661. doi:10.1016/j.marpetgeo.2018.09.025
- Li, J., Wen, X. Y., and Huang, C. M. (2016c). Lower cretaceous paleosols and paleoclimate in Sichuan Basin, China. *Cretac. Res.* 62, 154–171. doi:10.1016/j.cretres.2015.10.002
- Li, J. Z., Dong, D. Z., Chen, G. S., Wang, S. Q., and Chen, K. M. (2009). Prospects and strategic position of shale gas Resources in China. *Nat. Gas. Ind.* 29 (5), 11–16. (in Chinese with English Abstract). doi:10.3787/j.issn.1000.0976.2009.05.003
- Li, M. X., Liang, B., Wang, Q. W., Zhu, B., Hao, X. F., Ying, L. C., et al. (2013). Geochemistry of cretaceous argillaceous rocks in longquan mountain, western sichuan. *Geol. J. China Univ.* 19 (2), 346–354.
- Li, Q. H., Zhang, Y. X., Zhang, K. J., Yan, L. L., Zeng, L., Jin, X., et al. (2017). Garnet amphibolites from the ganzhi-litang fault zone, eastern Tibetan plateau: Mineralogy, geochemistry, and implications for evolution of the eastern paleo-tethys realm. *Int. Geol. Rev.* 60, 1954–1967. doi:10.1080/00206814.2017.1396563
- Li, R. B., Pei, X. Z., Liu, Z. Q., Li, Z. C., Ding, S. P., Liu, Z. G., et al. (2010a). Basin-Mountain coupling relationship of foreland basins between Dabashan and northeastern Sichuan—the evidence from LA-ICP-MS U-Pb dating of the detrital zircons. *Acta Geol. Sin.* 84, 1118–1134. (in Chinese with English abstract). doi:10.19762/j.cnki.dizhixuebao.2010.08.005
- Li, R. W., Li, C., Jiang, M. S., Sun, S., Jin, F. Q., and Zhang, W. H. (2000). Composition of clastic garnet in the Hefei Basin and its significance to source restoration and stratigraphic correlation. *Sci. China (Series D)*. 30, 91–98. (in Chinese with English abstract).
- Li, W., Yang, J. L., Jiang, J. W., Liu, J. M., and Liu, Z. C. (2009). Origin of upper triassic formation water in middle Sichuan Basin and its natural gas significance. *Petroleum Explor. Dev.* 36 (4), 428–435. doi:10.1016/s1876-3804(09)60138-5
- Li, X. H., Li, Z. X., Zhou, H. W., Liu, Y., and Kinny, P. D. (2002). U-Pb zircon geochronology, geochemistry and Nd isotopic study of neoproterozoic bimodal volcanic rocks in the Kangdian rift of Southsouth China: Implications for the initial rifting of rodonia. *Precambrian Res.* 113, 135–154. doi:10.1016/s0301-9268(01)00207-8
- Li, Y., Allen, P. A., Densmore, A. L., and Xu, Q. (2003). Evolution of the longmen Shan foreland basin (western sichuan, China) during the late triassic indosinian orogeny. *Basin Res.* 15, 117–138. doi:10.1046/j.1365-2117.2003.00197.x
- Li, Y. L., and Ji, X. T. (1993). Petrological character of Daxi conglomerate in Lushan-Tianquan and its provenance. *J. Mineral Petrol* 13 (3), 68–73. (in Chinese with English abstract). doi:10.19719/j.cnki.1001-6872.1993.03.011
- Li, Y. Q., He, D. F., Chen, L. B., Mei, Q. H., Li, C. X., and Zhang, L. (2016a). Cretaceous sedimentary basins in sichuan, SW China: Restoration of tectonic and depositional environments. *Cretac. Res.* 57, 50–65. doi:10.1016/j.cretres.2015.07.013
- Li, Y. Q., He, D. F., Li, D., Lu, R. Q., Fan, C., Sun, Y. P., et al. (2018). Sedimentary provenance constraints on the jurassic to cretaceous paleogeography of Sichuan Basin, SW China. *Gondwana Res.* 60, 15–33. doi:10.1016/j.gr.2018.03.015
- Li, Y. Q., He, D. F., Li, D., Wen, Z., Mei, Q. H., Li, C. X., et al. (2016b). Detrital zircon U-Pb geochronology and provenance of Lower Cretaceous sediments: Constraints for the northwestern Sichuan pro-foreland basin. *Palaeogeogr. Palaeoclimatol. Palaeoecol.* 453, 52–72. doi:10.1016/j.palaeo.2016.03.030
- Li, Y. W. (1979). Discovery of cretaceous brackish-water foraminifera and ostracoda in the Sichuan Basin, and their significance. *Geol. Rev.* 25 (1), 2–9. (in Chinese with English abstract). doi:10.16509/j.georeview.1979.01.002
- Li, Y. W. (1982). “Late jurassic-paleogene ostracods in Sichuan Basin, and their significance of stratigraphy,” in *Continental mesozoic stratigraphy and paleontology in Sichuan Basin of China, Part II, paleontological professional papers, 274-345* (Chengdu, China: People’s Publishing House of Sichuan). (in Chinese with English abstract).
- Li, Y. W. (1983). On the non-marine jurassic-cretaceous boundary in Sichuan Basin by ostracoda. *Bull. Chengdu Inst. Geol. Min. Res. Chin. Acad. Geol. Sci.* 4, 77–89. (in Chinese with English abstract). doi:10.16509/j.georeview.1983.05.013
- Li, Y. W. (1988). The application of ostracoda to the location of the non-marine jurassic-cretaceous boundary in the sichuan basin of China. *Dev. Palaeontol. Stratigr.* 11, 1245–1260.

- Li, Y. W. (1987). The cretaceous geological history of the Sichuan Basin. *Regional Geol. China* 1, 51–56. (in Chinese with English abstract).
- Li, Z. W., Chen, H. D., Liu, S. G., Hou, M. C., and Deng, B. (2010b). Differential uplift driven by thrusting and its lateral variation along the Longmenshan belt, Western Sichuan, China: Evidence from fission track thermochronology. *Chin. J. Geol.* 45 (4), 944–968. (in Chinese with English abstract).
- Li, Z. W., Liu, S. G., Chen, H. D., Deng, B., Hou, M. C., Wu, W. H., et al. (2012). Spatial variation in Mesozoic exhumation history of the Longmen Shan thrust belt (eastern Tibetan plateau) and the adjacent western Sichuan Basin: Constraints from fission track thermochronology. *J. Asian Earth Sci.* 47 (1), 185–203. doi:10.1016/j.jseas.2011.10.016
- Li, Z. W., Liu, S. G., Chen, H. D., Liu, S., Guo, B., and Tian, X. B. (2008). Structural segmentation and zonation and differential deformation across and along the Longmen thrust belt, west Sichuan, China. *J. Chengdu Univ. Technol. Sci. Technol. Ed.* 35, 440–455. (in Chinese with English abstract). doi:10.3969/j.issn.1671-9727.2008.04.0440.15
- Li, Z. X., Li, X. H., Kinny, P. D., Wang, J., Zhang, S., and Zhou, H. (2003). Geochronology of neoproterozoic syn-rift magmatism in the yangtze craton, south China and correlations with other continents: Evidence for a mantle superplume that broke up rodonia. *Precambrian Res.* 122, 85–109. doi:10.1016/s0301-9268(02)00208-5
- Li, Z. X., Li, X. H., Zhou, H. W., and Kinny, P. D. (2002). Grenvillian continental collision in south China: New SHRIMP U–Pb zircon results and implications for the configuration of rodonia. *Geology* 30, 163–166. doi:10.1130/0091-7613(2002)030<0163:gcisc>2.0.co;2
- Lin, M. B., Gou, Z. H., Wang, G. Z., Deng, J. H., Li, Y., Wang, D. Y., et al. (1996). *A research on the Orogenic model of Longmen mountains orogenic belt*. Chengdu: Press of Chengdu University of Science and Technology. (in Chinese with English abstract).
- Lin, M. B. (2008). The huge Wenchaun earthquake and Longmen tectonic belt. *J. Chengdu Univ. Technol. Sci. Technol. Ed.* 35 (4), 366–370. (in Chinese with English abstract).
- Linka, K. M., and Stawikowski, W. (2013). Garnet and tourmaline as provenance indicators of terrigenous material in epicontinental carbonates (Middle Triassic, S Poland). *Sediment. Geol.* 291 (4), 27–47. doi:10.1016/j.sedgeo.2013.03.005
- Liu, S. G., Deng, B., Jansa, L., Li, Z. W., Sun, W., Wang, G. Z., et al. (2018). Multi-stage basin development and hydrocarbon accumulations: A review of the sichuan basin at eastern margin of the Tibetan plateau. *J. Earth Sci.* 29 (2), 307–325. doi:10.1007/s12583-017-0904-8
- Liu, S. G., Deng, B., Jansa, L., Wang, G. Z., Li, X. H., Wang, C. S., et al. (2013b). Late triassic thickening of the songpan-ganzi triassic flysch at the edge of the northeastern Tibetan plateau. *Int. Geol. Rev.* 55 (16), 2008–2015. doi:10.1080/00206814.2013.812705
- Liu, S. G., Deng, B., Li, Z. W., Jansa, L., Liu, S., Wang, G. Z., et al. (2013a). Geological evolution of the longmenshan intracontinental composite orogen and the eastern margin of the Tibetan plateau. *J. Earth Sci.* 24 (6), 874–890. doi:10.1007/s12583-013-0391-5
- Liu, S. G., Luo, Z. L., Zhao, X. K., Xu, G. S., Wang, G. Z., and Zhang, C. J. (2003). Coupling relationships of sedimentary basin-orogenic belt systems and their dynamic models in west China. *Acta Geol. Sin.* 77 (2), 177–186. (in Chinese with English abstract).
- Liu, S. G., Sun, W., Li, Z. W., Deng, B., and Liu, S. (2008). Tectonic uplifting and gas pool formation since late cretaceous epoch, Sichuan Basin. *Nat. Gas. Geosci.* 19 (3), 293–300. (in Chinese with English Abstract). doi:10.11764/j.issn.1672-1926.2008.03.0293.08
- Liu, S. G. (1993). *The Formation and evolution of longmenshan thrust zone and western sichuan*. ChinaChengdu: Press of Chengdu University of Science and Technology.
- Liu, S., Li, Z., Kamp, P. J. J., Ran, B., Li, J., Deng, B., et al. (2019). Discovery of the Mesozoic Zoige paeo-plateau in eastern Tibetan Plateau and its geological significance. *J. Chengdu Univ. Technol. Sci. Technol. Ed.* 46 (1), 1–28. (in Chinese with English abstract). doi:10.3969/j.issn.1671-9727.2019.01.01
- Liu, W. Z. (2006). The Formation age and tectonic setting of the kangding complex in the western margin of the yangtze block. *J. Anhui Univ. Sci. Technol. Nat. Sci.* 26 (4), 1–5. (in Chinese with English abstract). doi:10.3969/j.issn.1672-1098.2006.04.0001.05
- Liu, X., Zhan, Q. Y., Zhu, D. C., Wang, Q., Xie, J. C., and Zhang, L. L. (2021). Provenance and tectonic uplift of the Upper Triassic strata in the southern Songpan-Ganzi fold belt, SW China: Evidence from detrital zircon geochronology and Hf isotope. *Acta Petrol. Sin.* 37 (11), 3513–3526. (in Chinese with English abstract). doi:10.18654/1000-0569/2021.11.16
- Liu-Zeng, J., Zhang, J. Y., McPhillips, D., Reiners, P., Wang, W., Pik, R., et al. (2018). Multiple episodes of fast exhumation since Cretaceous in southeast Tibet, revealed by low-temperature thermochronology. *Earth Planet. Sci. Lett.* 490, 62–76. doi:10.1016/j.epsl.2018.03.011
- Löwen, A. K., Meinhold, G., and Gungör, T. (2018). Provenance and tectonic setting of carboniferous–triassic sandstones from the karaburun peninsula, Western Turkey: A multi-method approach with implications for the palaeotethys evolution. *Sediment. Geol.* 375, 232–255. doi:10.1016/j.sedgeo.2017.11.006
- Ludwig, K. R. (2003). *User's manual for isoplot/ex v3.0a geochronology toolkit for microsoft excel*. Berkely: Berkeley Geochronological Center Special Publications, 25–31.
- Luo, L., Qi, J. F., Zhang, M. Z., Wang, K., and Han, Y. Z. (2014). Detrital zircon U–Pb ages of late triassic–late jurassic deposits in the Western and northern Sichuan Basin margin: Constraints on the foreland basin provenance and tectonic implications. *Int. J. Earth Sci. Geol. Rundsch.* 103, 1553–1568. doi:10.1007/s00531-014-1032-7
- Lv, F., Ran, B., Liu, S. G., Wang, Z. J., Sun, T., Li, X. H., et al. (2022). Provenance of the Lower Jurassic quartz-rich conglomerate in northwestern sichuan basin and its link with the pre-collisional unroofing history of the northlongmen Shan thrust belt, NE Tibetan plateau margin. *Front. Earth Sci.* 10, 982354. doi:10.3389/feart.2022.982354
- Mange, M. A., and Maurer, H. F. W. (1992). *Heavy minerals in colour*. London: Chapman & Hall, 147.
- Mange, M. A., and Morton, A. C. (2007). “Chapter 13 geochemistry of heavy minerals,” in *Developments in sedimentology*. Editors A. M. Maria and T. W. David (Elsevier), 345–391.
- Mange, M. A. (2002). *16th international sedimentological congress*. South Africa: Rand Afrikaans University, 34. New look at heavy minerals—A short course
- Meng, Q. R., Wang, E. Q., and Hu, J. M. (2005). Mesozoic sedimentary evolution of the northwest Sichuan basin: Implication for continued clockwise rotation of the southsouth China block. *GSA Bull.* 117, 396. doi:10.1130/B25407.1
- Ministry of Geology and Mineral Resources (1991). *Regional geology of sichuan province*. Beijing: Geological Publishing House, 1–689. (in Chinese with English abstract).
- Morton, A. C. (1985). A new approach to provenance studies: Electron microprobe analysis of detrital garnets from middle jurassic sandstones of the northern north sea. *Sedimentology* 32, 553–566. doi:10.1111/j.1365-3091.1985.tb00470.x
- Morton, A. C., Hallsworth, C. R., and Chalton, B. (2004). Garnet compositions in scottish and Norwegian basement terrains: A framework for interpretation of north sea sandstone provenance. *Mar. Petrol. Geol.* 21, 393–410. doi:10.1016/j.marpetgeo.2004.01.001
- Morton, A. C., and Hallsworth, C. R. (1994). Identifying provenance specific features of detrital heavy mineral assemblages in sandstones. *Sediment. Geol.* 90, 241–256. doi:10.1016/0037-0738(94)90041-8
- Morton, A. C., and Hallsworth, C. R. (1999). Processes controlling the composition of heavy mineral assemblages in sandstones. *Sediment. Geol.* 124, 3–29. doi:10.1016/s0037-0738(98)00118-3
- Morton, A. C., Whitham, A. G., and Fanning, C. M. (2005). Provenance of late cretaceous to paleocene submarine fan sandstones in the Norwegian sea: Integration of heavy mineral, mineral chemical and zircon age data. *Sediment. Geol.* 182, 3–28. doi:10.1016/j.sedgeo.2005.08.007
- Morton, A., Knox, R., and Frei, D. (2016). Heavy mineral and zircon age constraints on provenance of the sherwood sandstone group (Triassic) in the eastern Wessex basin, UK. *Proc. Geol. Assoc.* 127 (4), 514–526. doi:10.1016/j.pgeola.2016.06.001
- Mu, H. X., Yan, D. P., Qiu, L., Yang, W. X., Kong, R. Y., Gong, L. X., et al. (2019). formation of the late triassic Western sichuan foreland basin of the qinling orogenic belt, SW China: Sedimentary and geochronological constraints from the Xujiahe Formation. *J. Asian Earth Sci.* 183, 103938. doi:10.1016/j.jseas.2019.103938
- Mulch, A., and Chamberlain, C. P. (2006). The rise and growth of Tibet. *Nature* 439, 670–671. doi:10.1038/439670a
- Najman, Y., and Garzanti, E. (2000). Reconstructing early Himalayan tectonic evolution and paleogeography from Tertiary foreland basin sedimentary rocks, northern India. *Geol. Soc. Am. Bull.* 112 (3), 435–449. doi:10.1130/0016-7606(2000)112<435:rehtea>2.0.co;2
- Nichols, G. (2009). *Sedimentology and stratigraphy*. John Wiley & Sons.
- Otofujii, Y., Inoue, Y., Funahara, S., Murata, F., and Zheng, X. (1990). Palaeomagnetic study of eastern tibet-deformation of the three rivers region. *Geophys. J. Int.* 103, 85–94. doi:10.1111/j.1365-246x.1990.tb01754.x
- Panaiotu, C. E., Vasiliev, I., Panaiotu, C. G., Krijgsman, W., and Langereis, C. G. (2007). Provenance analysis as a key to orogenic exhumation: A case study from the East carpathians (Romania). *Terra nova*. 19 (2), 120–126. doi:10.1111/j.1365-3121.2006.00726.x
- Pettijohn, F. J., Potter, P. E., and Siever, R. (1987). *Sand and sandstone*. third ed. New York: Springer.
- Qian, T., Liu, S. F., Li, W. P., Gao, T. J., and Chen, X. L. (2015). Early–middle jurassic evolution of the northern yangtze foreland basin: A record of uplift following triassic continent–continent collision to form the qinling–dabieshan orogenic belt. *Int. Geol. Rev.* 57, 327–341. doi:10.1080/00206814.2015.1006270
- Rahl, J. M., Harbor, D. J., Galli, C. I., and O'Sullivan, P. (2018). Foreland basin record of uplift and exhumation of the Eastern Cordillera, northwest Argentina. *Tectonics* 37, 4173–4193. doi:10.1029/2017TC004955
- Reid, A. J., Fowler, A. P., Phillips, D., and Wilson, C. J. L. (2005). Thermochronology of the Yidun arc, central eastern Tibetan plateau: Constraints from 40Ar/39Ar K-feldspar and apatite fission track data. *J. Asian Earth Sci.* 25, 915–935. doi:10.1016/j.jseas.2004.09.002
- Reid, A., Wilson, C. J. L., Shun, L., Pearson, N., and Belousova, E. (2007). Mesozoic plutons of the Yidun arc, SW China: U/Pb geochronology and Hf isotopic signature. *Ore Geol. Rev.* 31 (1–4), 88–106. doi:10.1016/j.oregeorev.2004.11.003
- Richardson, N. J., Densmore, A. L., Seward, D., Fowler, A., Wipf, M., Ellis, M. A., et al. (2008). Extraordinary denudation in the Sichuan Basin: Insights from low-temperature thermochronology adjacent to the eastern margin of the Tibetan plateau. *J. Geophys. Res.* 113 (B4), B044409. doi:10.1029/2006jb004739
- Roger, F., Jolivet, M., and Malavieille, J. (2010). The tectonic evolution of the songpan garze (north tibet) and adjacent areas from proterozoic to present: A synthesis. *J. Asian Earth Sci.* 39, 254–269. doi:10.1016/j.jseas.2010.03.008
- Roger, F., Malavieille, J., Leloup, P. H., Calassou, S., and Xu, Z. (2004). Timing of granite emplacement and cooling in the Songpan-Garze Fold Belt (eastern Tibetan Plateau) with tectonic implications. *J. Asian Earth Sci.* 22 (5), 465–481. doi:10.1016/s1367-9120(03)00089-0
- Rohrmann, A., Kapp, P., Carrapa, B., Reiners, P. W., Gynn, J., Ding, L., et al. (2012). Thermochronologic evidence for plateau formation in central Tibet by 45 Ma. *Geology* 40, 187–190. doi:10.1130/g32530.1

- Rowley, D. B., and Currie, B. S. (2006). Palaeo-altimetry of the late eocene to miocene lunpola basin, central tibet. *Nature* 439, 677–681. doi:10.1038/nature04506
- Sabeen, H. M., Ramanujam, N., and Morton, A. C. (2002). The provenance of garnet: Constraints provided by studies of coastal sediments from southern India. *Sediment. Geol.* 152, 279–287. doi:10.1016/S0037-0738(02)00083-0
- Sevastjanova, I., Hall, R., and Alderton, D. (2012). A detrital heavy mineral viewpoint on sediment provenance and tropical weathering in SE Asia. *Sediment. Geol.* 280, 179–194. doi:10.1016/j.sedgeo.2012.03.007
- Shao, T. B., Cheng, N. F., and Song, M. S. (2016). Provenance and tectonic-paleogeographic evolution: Constraints from detrital zircon U–Pb ages of late triassic–early jurassic deposits in the northern Sichuan basin, central China. *J. Asian Earth Sci.* 127, 12–31. doi:10.1016/j.jseas.2016.05.027
- Shellnutt, J. G. (2014). The emeishan large igneous province: A synthesis. *Geosci. Front.* 5, 369–394. doi:10.1016/j.gsf.2013.07.003
- Shen, C. B., Mei, L. F., and Xu, S. H. (2009). Fission track dating of mesozoic sandstones and its tectonic significance in the eastern Sichuan Basin, China. *Radiat. Meas.* 44 (9/10), 945–949. doi:10.1016/j.radmeas.2009.10.001
- Shen, X. M., Tian, Y. T., Zhang, G. H., Zhang, S. M., Carter, A., Kohn, B. P., et al. (2019). Late Miocene hinterland crustal shortening in the Longmen Shan thrust belt, the eastern margin of the Tibetan Plateau. *J. Geophys. Res. Solid Earth* 124 (11), 11972–11991. doi:10.1029/2019jb018358
- Shi, Z. S., Wang, X. Q., and Wu, C. J. (2011). The heavy minerals and provenances of the upper triassic Xujiahe Formation in Sichuan Basin. *Nat. Gas. Geosci.* 22 (4), 618–627. (in Chinese with English Abstract).
- Sichuan Bureau of Geology and Mineral Resources (SBGMR) (1997). *Stratigraphy (lithostratic) of sichuan province*. Wuhan: China University of Geosciences Press.
- Sichuan Bureau of Geology and Mineral Resources (SBGMR) (1982). “Writing group of continental mesozoic stratigraphy and paleontology,” in *Continental mesozoic stratigraphy and paleontology in sichuan basin of China*. Editor S. Basin (Chengdu: People’s Publishing House of Sichuan), 622–179 (in Chinese).
- Sichuan Bureau of Geology and Mineral Resources (SBGMR) (1993). *Report of 1: 50,000 tianquan and lingguan regional geological survey*. Chengdu: Chengdu University of Technology.
- Smyth, H. R., Hall, R., and Nichols, G. J. (2008). Significant volcanic contribution to some quartz-rich sandstones, east java, Indonesia. *J. Sediment. Res.* 78 (5), 335–356. doi:10.2110/jsr.2008.039
- Spicer, R. A., Su, T., Valdes, P. J., Farnsworth, A., Wu, F. X., Shi, G., et al. (2021). Why ‘the uplift of the Tibetan Plateau’ is a myth? *Nat. Sci. Rev.* 8 (1), nwa091. doi:10.1093/nsr/nwa091
- Su, D. Z. (1983). Note on a new lepidotes from the cretaceous of sichuan. *Vertebr. Palasiat.* 21 (3), 177–185. (in Chinese with English abstract).
- Sun, W. H., Zhou, M. F., Gao, J. F., Yang, Y. H., Zhao, X. F., and Zhao, J. H. (2009). Detrital zircon U–Pb geochronological and Lu–Hf isotopic constraints on the Precambrian magmatic and crustal evolution of the Western Yangtze Block, SW China. *Precambrian Res.* 172, 99–126. doi:10.1016/j.precamres.2009.03.010
- Sun, W. H., Zhou, M. F., and Zhao, J. H. (2007). Geochemistry and tectonic significance of basaltic lavas in the neoproterozoic yanbian group, southern sichuan province, southwest China. *Int. Geol. Rev.* 49, 554–571. doi:10.2747/0020-6814.49.6.554
- Tan, X. B., Liu, Y. D., Lee, Y. H., Lu, R. Q., Xu, X. W., Suppe, J., et al. (2019). Parallelism between the maximum exhumation belt and the Moho ramp along the eastern Tibetan Plateau margin: Coincidence or consequence? *Earth Planet. Sci. Lett.* 507, 73–84. doi:10.1016/j.epsl.2018.12.001
- Tan, X. B., Xu, X. W., Lee, Y. H., Lu, R. Q., Xu, C., Li, K., et al. (2017). Late Cenozoic thrusting of major faults along the central segment of Longmen Shan, eastern Tibet: Evidence from low-temperature thermochronology. *Tectonophysics* 712–713, 145–155. doi:10.1016/j.tecto.2017.05.016
- Tang, Y., Zhang, Y., and Tong, L. (2017). Provenance of middle to late triassic sedimentary rocks in the zoige depression in the ne part of the songpan-ganzi flysch basin: Petrography, heavy minerals, and zircon U–Pb geochronology. *Geol. J.* 52, 449–462. doi:10.1002/gj.3001
- Teraoka, Y., Suzuki, M., Hayashi, T., and Kawakami, K. (1997). Detrital garnets from paleozoic and mesozoic sandstones in the onogawa area, east kyushu, southwest Japan. *Bull. Fac. Educ. Hiroshima Univ.* 19, 87–101.
- Teraoka, Y., Suzuki, M., and Kawakami, K. (1998). Provenance of cretaceous and Paleogene sediments in the median zone of southwest Japan. *Bull. Geol. Surv. Jpn.* 49, 395–411.
- Tian, Q. (2018). *Provenance analysis of the lower jurassic baitianba Formation in northwestern Sichuan Basin and its tectonic significance*. Master’s thesis. Chengdu, China: Chengdu University of Technology, 1–81. (in Chinese with English abstract).
- Tian, Y. T., Kohn, B. P., Gleadow, A. J. W., and Hu, S. B. (2014a). A thermochronological perspective on the morphotectonic evolution of the southeastern Tibetan Plateau. *J. Geophys. Res. Solid Earth* 119 (1), 676–698. doi:10.1002/2013jb010429
- Tian, Y. T., Kohn, B. P., Gleadow, A. J. W., and Hu, S. B. (2013). Constructing the Longmen Shan eastern Tibetan Plateau margin: Insights from low-temperature thermochronology. *Tectonics* 32, 576–592. doi:10.1002/tect.20043
- Tian, Y. T., Kohn, B. P., Hu, S. B., and Gleadow, A. J. W. (2014b). Postorogenic rigid behavior of the eastern Songpan-Ganze terrane: Insights from low-temperature thermochronology and implications for intracontinental deformation in central Asia. *Geochem. Geophys. Geosystems* 15 (2), 453–474. doi:10.1002/2013gc004951
- Tian, Y. T., Li, R., Tang, Y., Xu, X., Wang, Y. J., and Zhang, P. Z. (2018). Thermochronological constraints on the late Cenozoic morphotectonic evolution of the Min Shan, the eastern margin of the Tibetan Plateau. *Tectonics* 37, 1733–1749. doi:10.1029/2017tc004868
- Tian, Z. D., Leng, C. B., Zhang, X. C., Yin, C. J., Zhang, W., Cuo, J. H., et al. (2018). Mineralogical and petrogeochemical characteristics of the metamorphic basement of Yidun terrane and their geological implication. *Acta Mineral. Sin.* 38 (2), 152–165. (in Chinese with English abstract).
- Tong, C. G. (1992). *Tectonic evolution of Sichuan Basin and gas/oil accumulation*. Beijing: Geological Publishing House.
- van Hattum, M. W. A., Hall, R., Pickard, A. L., and Nichols, G. J. (2006). Southeast asian sediments not from asia: Provenance and geochronology of north borneo sandstones. *Geology* 34, 589–592. doi:10.1130/g21939.1
- Veevers, J. J., and Saeed, A. (2013). Age and composition of Antarctic sub-glacial bedrock reflected by detrital zircons, erratics, and recycled microfossils in the Ellsworth Land–Antarctic Peninsula–Weddell Sea–Dronning Maud Land sector (240°E–0°–015°E). *Gondwana Res.* 23, 296–332. doi:10.1016/j.gr.2012.05.010
- Wallis, S., Tsujimori, T., Aoya, M., Kawakami, T., Terada, K., Suzuki, K., et al. (2003). Cenozoic and mesozoic metamorphism in the longmenshan orogen: Implications for geodynamic models of eastern tibet. *Geology* 31 (9), 745–748. doi:10.1130/g19562.1
- Wang, B. Q., Wang, W., Chen, W. T., Gao, J. F., Zhao, X. F., Yan, D. P., et al. (2013). Constraints of detrital zircon U–Pb ages and Hf isotopes on the provenance of the Triassic Yidun Group and tectonic evolution of the Yidun Terrane, eastern Tibet. *Sediment. Geol.* 289, 74–98. doi:10.1016/j.sedgeo.2013.02.005
- Wang, C. S., Zhao, X. X., Liu, Z. F., Lippert, P. C., Graham, S. A., Coe, R. S., et al. (2008). Constraints on the early uplift history of the Tibetan Plateau. *Proc. Natl. Acad. Sci. U. S. A.* 105, 4987–4992. doi:10.1073/pnas.0703595105
- Wang, E., Kirby, E., Furlong, K. P., van Soest, M., Xu, G., Shi, X., et al. (2012). Two-phase growth of high topography in eastern Tibet during the Cenozoic. *Nat. Geosci.* 5, 640–645. doi:10.1038/ngeo1538
- Wang, L. C., Shen, L. J., Liu, C. L., Chen, K., Ding, L., and Wang, C. S. (2021). The late cretaceous source-to-sink system at the eastern margin of the Tibetan plateau: Insights from the provenance of the lanping basin. *Geosci. Front.* 12, 101102. doi:10.1016/j.gsf.2020.11.002
- Wang, L. J., Yu, J. H., Griffin, W. L., and O’Reilly, S. Y. (2012). Early crustal evolution in the Western yangtze block: Evidence from U–Pb and Lu–Hf isotopes on detrital zircons from sedimentary rocks. *Precambrian Res.* 222–223, 368–385. doi:10.1016/j.precamres.2011.08.001
- Wang, Q. C. (2013). Erosion and sedimentary record of orogenic belt. *Chin. J. Geol.* 48 (1), 1–31. (in Chinese with English abstract).
- Wang, Q. W., Kan, Z. Z., Liang, B., and Zeng, Y. J. (2006). Stratigraphic division and correlation of the continental meso-cenozoic group in ya’an, west Sichuan Basin. *Acta Geol. Sichuan* 26 (2), 65–69. (in Chinese with English abstract).
- Wang, Z. B., Yang, S. Y., Mei, X., and Lu, K. (2018). Detrital garnet chemistry of the Changjiang (Yangtze River) sediments and their provenance implication. *J. Tongji Univ. Nat. Sci.* 46 (10), 1455–1472.
- Wei, M. (1979). Ostracoda and geological age of the Tianmashan Formation in sichuan. *Geol. Rev.* 25 (02), 7–14.
- Weislogel, A. L., Graham, S. A., Chang, E. Z., Wooden, J. L., and Gehrels, G. E. (2010). Detrital zircon provenance from three turbidite depocenters of the Middle-Upper Triassic Songpan–Ganzi complex, central China: Record of collisional tectonics, erosional exhumation, and sediment production. *Geol. Soc. Am. Bull.* 122 (11–12), 2041–2062. doi:10.1130/b26606.1
- Weislogel, A. L., Graham, S. A., Chang, E. Z., Wooden, J. L., Gehrels, G. E., and Yang, H. (2006). Detrital zircon provenance of the late triassic songpan-ganzi complex: Sedimentary record of collision of the north and south China blocks. *Geology* 34, 97–100. doi:10.1130/g21929.1
- Weislogel, A. L. (2008). Tectonostratigraphic and geochronologic constraints on evolution of the northeast Paleotethys from the Songpan–Ganzi complex, central China. *Tectonophysics* 451, 331–345. doi:10.1016/j.tecto.2007.11.053
- Weltje, G. J., and Eynatten, H. V. (2004). Quantitative provenance analysis of sediments: Review and outlook. *Sediment. Geol.* 171 (1/4), 1–11. doi:10.1016/j.sedgeo.2004.05.007
- Wiedenbeck, M., Hanchar, J. M., Peck, W. H., Sylvester, P., Valley, J., Whitehouse, M., et al. (2004). Further characterisation of the 91500 zircon crystal. *Geostand. Geoanalytical Res.* 28 (1), 9–39. doi:10.1111/j.1751-908x.2004.tb01041.x
- Wilson, C. J. L., Harrowfield, M. J., and Reid, A. J. (2006). Brittle modification of triassic architecture in eastern tibet: Implications for the construction of the cenozoic plateau. *J. Asian Earth Sci.* 27, 341–357. doi:10.1016/j.jseas.2005.04.004
- Worley, B. A., and Wilson, C. J. L. (1996). Deformation partitioning and foliation reactivation during transpressional orogenesis, an example from the Central Longmen Shan, China. *J. Struct. Geol.* 18, 395–411. doi:10.1016/0191-8141(95)00095-u
- Worley, B. A., Wilson, C. J. L., Liu, S. G., and Luo, Z. L. (1995). Structural observations from the wenchuan-maowen metamorphic belt, longmen mountains, China. *J. Chengdu Inst. Technol. Nat. Sci.* 22 (1), 24–41.
- Wright, W. I. (1938). The composition and occurrence of garnets. *Am. Mineral.* 23, 436–449.

- Wu, L., Xiao, A., Yang, S., Wang, L., Mao, L., Wang, L., et al. (2012). Two stage evolution of the altn tagh fault during the cenozoic: New insight from provenance analysis of a geological section in NW qaidam basin, NW China. *Terra nova*. 24 (5), 387–395. doi:10.1111/j.1365-3121.2012.01077.x
- Xu, G., and Kamp, P. J. J. (2000). Tectonics and denudation adjacent to the Xianshuihe Fault, eastern Tibetan Plateau: Constraints from fission track thermochronology. *J. Geophys. Res.* 105, 19231–19251. doi:10.1029/2000jb900159
- Xu, Z. Q., Fu, X. F., Ma, X. X., Qi, X. X., Wu, C., Hou, L. W., et al. (2016). The gneiss domes in Tibetan Plateau and their potential for prospecting. *Acta Geol. Sin.* 90 (11), 2971–2981. (in Chinese with English abstract).
- Xu, Z. Q., Li, H. Q., Hou, L. W., Fu, X. F., Chen, W., Zeng, L. S., et al. (2007). Uplift of the Longmen–Jinping orogenic belt along the eastern margin of the Qinghai–Tibet Plateau: Large-scale detachment faulting and extrusion mechanism. *Geol. Bull. China* 26 (10), 1262–1276. (in Chinese with English abstract).
- Xu, Z. Q., Zhao, Z. B., Peng, M., Ma, X. X., Li, H. Q., and Zhao, J. M. (2016). Review of “orogenic plateau”. *Acta Petrol. Sin.* 32 (12), 3557–3571. (in Chinese with English abstract).
- Xue, Z. H., Lin, W., Chu, Y., Faure, M., Chen, Y., Ji, W. B., et al. (2021). An intracontinental orogen exhumed by basement-slice imbrication in the Longmenshan Thrust Belt of the Eastern Tibetan Plateau. *Geol. Soc. Am. Bull.* 134, 15–38. doi:10.1130/B35826.1
- Xue, Z. H., Martelet, G., Lin, W., Faure, M., Chen, Y., Wei, W., et al. (2017). Mesozoic crustal thickening of the Longmenshan belt (NE Tibet, China) by imbrication of basement slices: Insights from structural analysis, petrofabric and magnetic fabric studies, and gravity modeling. *Tectonics* 36 (3–4), 3110–3134. doi:10.1002/2017tc004754
- Yan, D. P., Zhou, M. F., Li, S. B., and Wei, G. Q. (2011). Structural and geochronological constraints on the Mesozoic–Cenozoic tectonic evolution of the Longmen Shan thrust belt, eastern Tibetan Plateau. *Tectonics* 30. doi:10.1029/2011TC002867
- Yan, D. P., Zhou, M. F., Wei, G. Q., Gao, J. F., Liu, S. F., Xu, P., et al. (2008). The pengguan tectonic dome of longmen mountains, sichuan province: Mesozoic denudation of a neoproterozoic magmatic arc-basin system. *Sci. China Ser. D-Earth Sci.* 51, 1545–1559. doi:10.1007/s11430-008-0126-0
- Yan, Z., Guo, X. Q., Fu, C. L., Aitchison, J., Wang, Z. Q., and Li, J. L. (2014). Detrital heavy mineral constraints on the triassic tectonic evolution of the West qinling terrane, NW China: Implications for understanding subduction of the paleotethyan ocean. *J. Geol.* 122, 591–608. doi:10.1086/677264
- Yan, Z. K., Tian, Y. T., Li, R., Vermeesch, P., Sun, X. L., Li, Y., et al. (2019). Late triassic tectonic inversion in the upper yangtze block: Insights from detrital zircon u–pb geochronology from south-Western sichuan basin. *Basin Res.* 31, 92–113. doi:10.1111/bre.12310
- Yang, G. C., Yu, B. S., Chen, J. Q., Yao, J. M., Li, S. Y., and Wu, Y. H. (2010). Geochemical research on rare Earth elements of argillaceous rocks of upper jurassic and cretaceous in the western sichuan foreland basin. *Geoscience* 24 (1), 140–149. (in Chinese with English abstract).
- Yang, L., Yuan, W. M., Zhu, X. Y., and Shi, Z. (2019). Late triassic-cenozoic thermochronology in the southern sanjiang tethys, SW China, new insights from zircon fission track analysis. *J. Earth Sci.* 30 (5), 996–1004. doi:10.1007/s12583-019-1014-6
- Ye, C. H. (1983). Cretaceous ostracod assemblages in Sichuan Basin, southwest China. *Acta Palaeontol. Sin.* 22 (02), 204–208.
- Yuan, H. L., Gao, S., Dai, M. N., Zong, C. L., Günther, D., Fontaine, G. H., et al. (2007). Simultaneous determinations of U–Pb age, Hf isotopes and trace element compositions of zircon by excimer laser-ablation quadrupole and multiple-collector ICP-MS. *Chem. Geol.* 247, 100–118. doi:10.1016/j.chemgeo.2007.10.003
- Zeng, Y. J., Yang, X. J., Li, Y. Q., Xie, Q. X., Zhu, B., and Hao, X. F. (2004). Tectonic significance of meso-cenozoic conglomerate in the south of the West sichuan foreland basin. *Acta Geol. Sichuan* 22 (4), 198–201.
- Zhang, H. F., Parrish, R., Zhang, L., Xu, W. C., Yuan, H. L., Gao, S., et al. (2007). A-type granite and adakitic magmatism association in Songpan–Garze fold belt, eastern Tibetan Plateau: Implication for lithospheric delamination. *Lithos* 97, 323–335. doi:10.1016/j.lithos.2007.01.002
- Zhang, K. J., Li, B., Wei, Q. G., Cai, J. X., and Zhang, Y. X. (2008). Proximal provenance of the Western Songpan–Ganzi turbidite complex (Late Triassic, eastern Tibetan plateau): Implications for the tectonic amalgamation of China. *Sediment. Geol.* 208 (1), 36–44. doi:10.1016/j.sedgeo.2008.04.008
- Zhang, K. J., Li, B., and Wei, Q. G. (2012). Diversified provenance of the songpan-ganzi triassic turbidites, central China: Constraints from geochemistry and Nd isotopes. *J. Geol.* 120 (01), 69–82. doi:10.1086/662716
- Zhang, Y., Jia, D., Shen, L., Yin, H. W., Chen, Z. X., Li, H. B., et al. (2015). Provenance of detrital zircons in the late triassic sichuan foreland basin: Constraints on the evolution of the qinling orogen and longmen Shan thrustfold belt in central China. *Int. Geol. Rev.* 57, 1806–1824. doi:10.1080/00206814.2015.1027967
- Zhang, Y. L., Wang, Z. Q., Wang, G., Li, Q., and Lin, J. F. (2016). Chromian spinel, zircon age constraints on the provenance of early triassic feixianguan Formation sandstones. *Geol. Rev.* 62 (01), 54–72.
- Zhang, Y. X., Tang, X. C., Zhang, K. J., Tang, X. C., and Gao, C. L. (2014). U–Pb and Lu–Hf isotope systematics of detrital zircons from the Songpan–Ganzi Triassic flysch, NE Tibetan Plateau: Implications for provenance and crustal growth. *Int. Geol. Rev.* 56 (1), 29–56. doi:10.1080/00206814.2013.818754
- Zhang, Y. X., Zeng, L., Li, Z. W., Wang, C. S., Zhang, K. J., Yang, W. G., et al. (2015). Late permian–triassic siliciclastic provenance, palaeogeography, and crustal growth of the songpan terrane, eastern Tibetan plateau: Evidence from U–Pb ages, trace elements, and Hf isotopes of detrital zircons. *Int. Geol. Rev.* 57 (2), 159–181. doi:10.1080/00206814.2014.999356
- Zhao, J. H., and Zhou, M. F. (2007). Geochemistry of Neoproterozoic mafic intrusions in the Panzhihua district (Sichuan Province, SW China): Implications for subduction-related metasomatism in the upper mantle. *Precambrian Res.* 152, 27–47. doi:10.1016/j.precamres.2006.09.002
- Zhao, J. H., Zhou, M. F., Yan, D. P., Yang, Y. H., and Sun, M. (2008). Zircon Lu–Hf isotopic constraints on Neoproterozoic subduction-related crustal growth along the Western margin of the Yangtze Block, South China. *Precambrian Res.* 163, 189–209. doi:10.1016/j.precamres.2007.11.003
- Zhao, X. F., Zhou, M. F., Li, J. W., and Wu, F. Y. (2008). Association of neoproterozoic A- and I-type granites in south China: Implications for generation of A-type granites in a subduction-related environment. *Chem. Geol.* 257, 1–15. (in Chinese with English abstract). doi:10.1016/j.chemgeo.2008.07.018
- Zhou, M. F., Ma, Y. X., Yan, D. P., Xia, X. P., Zhao, J. H., and Sun, M. (2006a). The yanbian terrane (southern sichuan province, SW China): A neoproterozoic arc assemblage in the Western margin of the yangtze block. *Precambrian Res.* 144, 19–38. doi:10.1016/j.precamres.2005.11.002
- Zhou, M. F., Kennedy, A. K., Sun, M., Malpas, J., and Leshner, M. (2002b). Neoproterozoic Arc-Related mafic intrusions along the northern margin of South China: Implications for the accretion of rodonia. *J. Geol.* 110, 611–618. doi:10.1086/341762
- Zhou, M. F., Yan, D. P., Kennedy, A. K., Li, Y. Q., and Ding, J. (2002a). SHRIMP U–Pb zircon geochronological and geochemical evidence for Neoproterozoic arc-magmatism along the Western margin of the Yangtze Block, South China. *Earth Planet Sci. Lett.* 196, 51–67. doi:10.1016/s0012-821x(01)00595-7
- Zhou, M. F., Yan, D. P., Wang, C. L., Qi, L., and Kennedy, A. (2006b). Subduction-related origin of the 750 Ma xuelongbao adakitic complex (sichuan province, China): Implications for the tectonic setting of the giant neoproterozoic magmatic event in south China. *Earth Planet. Sci. Lett.* 248, 286–300. doi:10.1016/j.epsl.2006.05.032
- Zhu, C. Q., Hu, S. B., Qiu, N. S., Rao, S., and Yuan, Y. S. (2016). The thermal history of the Sichuan Basin, SW China: Evidence from the deep boreholes. *Sci. China (Earth Sci.)* 59, 70–82. doi:10.1007/s11430-015-5116-4
- Zhu, M., Chen, H., Zhou, J., and Yang, S. (2017). Provenance change from the middle to late triassic of the southwestern Sichuan basin, southwest China: Constraints from the sedimentary record and its tectonic significance. *Tectonophysics* 700–701, 92–107. doi:10.1016/j.tecto.2017.02.006
- Zhuang, Z. H., Tian, D. X., Ma, X. H., Ren, X. F., Jiang, X. C., and Xu, S. J. (1988). A paleomagnetic study along the yan-an-tian-quan cretaceous-eogene section in Sichuan Basin. *Geophys. Geochem. Explor.* 12 (03), 224–228.
- Zimmermann, S., and Hall, R. (2019). Provenance of Cretaceous sandstones in the Banda Arc and their tectonic significance. *Gondwana Res.* 67, 1–20. doi:10.1016/j.gr.2018.09.008
- Zimmermann, S., and Hall, R. (2016). Provenance of triassic and jurassic sandstones in the banda arc: Petrography, heavy minerals and zircon geochronology. *Gondwana Res.* 37, 1–19. doi:10.1016/j.gr.2016.06.001